International Journal of Engineering Science 78 (2014) 134–153

Contents lists available at ScienceDirect

International Journal of Engineering Science

journal homepage: www.elsevier.com/locate/ijengsci

Magneto-electro-elastic effective properties of multilayered artificial multiferroics with arbitrary lamination direction

S. Giordano [a,*], M. Goueygou [a], N. Tiercelin [a], A. Talbi [a], P. Pernod [a], V. Preobrazhensky [a,b]

[a] International Associated Laboratory LIA LEMAC/LICS: IEMN, UMR CNRS 8520, PRES Lille Nord de France, ECLille, 59651 Villeneuve d'Ascq, France
[b] Wave Research Center, Prokhorov General Physics Institute, Russian Academy of Science, 38 Vavilov str., Moscow 119991, Russia

ARTICLE INFO

Article history:
Received 17 October 2013
Received in revised form 28 January 2014
Accepted 11 February 2014

Keywords:
Multilayered materials
Multiferroics
Homogenization
Magneto-electro-elastic behavior

ABSTRACT

This work deals with the determination of the effective response of a multilayered or laminated heterostructure composed of materials with an arbitrary coupled anisotropic behavior. In particular, we elaborate a fully algebraic technique for obtaining the homogenized parameters of a magneto-electro-elastic system (artificial multiferroic). To do this, we load the system with an arbitrary electromagnetic/mechanical generalized action and we calculate the coupled physical fields within each layer. Then, we determine the average values of these fields, eventually obtaining the effective tensor response of the whole structure. The theory has been developed for an arbitrary lamination direction, taken into account by means of an *ad hoc* lamination tensor $\mathcal{P}_{\vec{n}}$ whose components are obtained in closed form. Its implementation is based on simple matrix algebra and does not require any extensive computation. Moreover, the formalism has been generalised to graded structures and to multiple-rank laminated materials.

1. Introduction

Magneto-electro-elastic composites and multiferroic phases represent a new class of materials with several potential applications in modern nanoscience and nanotechnology (Eerenstein, Mathur, & Scott, 2006; Fiebig, 2005; Nan, Bichurin, Dong, Viehland, & Srinivasan, 2008; Ramesh & Spaldin, 2007). Their peculiar characteristic is the cross-coupling between electric polarization and magnetization. This interaction offers new possibilities for functional electronic devices, such as sensors, actuators, transducers and memories (Wang, Hu, Lin, & Nan, 2010). Such materials can be realized through single phases or composite structures. However, because of the weak magneto-electric coupling (at very low temperature) of most single-phase systems (Lawes & Srinivasan, 2011), the introduction of composites offers a promising route for obtaining strong interactions at room temperature. In these materials, the magneto-electric coupling is strain or stress-mediated because of the magnetostrictive and piezoelectric properties of the components. From the historical point of view, one of the first sintered magnetoelectric composites was based on the combination $BaTiO_3$–$NiFe_2O_4$ with small additions of cobalt and manganese (van den Boomgaard & Born, 1978). More recently, laminated structures with a significant magnetoelectric coupling have been proposed and fabricated by Fetisov, Perov, Fetisov, Srinivasan, and Petrov (2011) and others based on film technology by Tiercelin et al. (2008a, 2008b). Several geometries have been thoroughly analysed from the theoretical point of view by Ramirez, Heyliger, and Pan (2006) and Kuo and Pan (2011). Such heterostructures are strongly indicated for

* Corresponding author. Address: Institut d'électronique de microélectronique et de nanotechnologie, UMR CNRS 8520, Laboratoire central, Cité scientifique, Avenue Henri Poincaré, CS 60069, 59652 Villeneuve d'Ascq cedex, France. Tel.: +33 03 20 19 79 58; fax: +33 03 20 19 79 84.
E-mail addresses: Stefano.Giordano@iemn.univ-lille1.fr, Stefano.Giordano@univ-lille1.fr (S. Giordano).
URL: http://www.giordanostefano.it (S. Giordano).

http://dx.doi.org/10.1016/j.ijengsci.2014.02.011
0020-7225/

achieving low-power devices. In fact, the electrical/mechanical reorientation of the magnetization dissipates a very small amount of energy and it is therefore appropriate for memories, spintronics and new paradigms of information processing (Dusch et al., 2013; Giordano, Dusch, Tiercelin, Pernod, & Preobrazhensky, 2012; Roy, Bandyopadhyay, & Atulasimha, 2011; Tiercelin et al., 2011).

In order to analyse and design materials and devices with magnetoelectric coupling, it is important to determine the distribution of the physical fields within these heterogeneous structures. In particular, nanomechanical techniques (Colombo & Giordano, 2011; Eshelby, 1957; Giordano & Palla, 2008; Kachanov & Sevostianov, 2005; Palla, Giordano, & Colombo, 2010) and homogenization schemes (Corcolle, Daniel, & Bouillault, 2008; Giordano, 2005, 2007; Huang & Kuo, 1997; Huang, Chiu, & Liu, 1998) play a central role for evaluating the effective magnetic, electric and elastic properties of composite systems. An exhaustive analysis of the theoretical modelling of magnetostrictive-piezoelectric nanostructures has been developed by Bichurin, Petrov, Averkin, and Liverts (2010a, 2010b). Although very efficient multi-scale computational techniques have been elaborated to homogenize the behavior of composite structures (Brenner, 2009), there is a great interest in working out analytical procedures providing their effective physical properties (Milton, 2004; Torquato, 2002). In fact, these theoretical approaches are not only stimulating for the encountered mathematical challenges, but also extremely competitive with numerical methods from the computational point of view. Another advantage of these approaches is the possibility to directly optimize some effective properties in terms of microstructural features, e.g. crystallographic orientations and volume fractions of constituents.

In this paper, we elaborate a theoretical methodology for determining the effective properties of multilayered magneto-electro-elastic heterostructures with an arbitrary lamination direction. This geometry is largely used in modern nanotechnology since, compared to a particulate composite, it exhibits much higher magneto-electric couplings, as discussed by Zhai, Xing, Dong, Li, and Viehland (2008).

As for the history of the analysis of laminates, the first pioneering results were obtained by Postma (1955) and Backus (1962) for the purely elastic case and by Tartar (1979) for the purely dielectric one. They developed a general method for determining the effective tensors in the absence of physical couplings and for a fixed lamination direction. Later, these results were generalized by Milton (1990) in order to consider an arbitrary direction of lamination. Furthermore, other techniques for dealing with piezoelectric and/or magnetoelastic laminated materials were introduced as well (Avellaneda & Harshé, 1994; Avellaneda & Olson, 1993; Gibiansky & Torquato, 1999). The so-called multiple-rank laminates (i.e. laminates of laminates) were introduced by Maxwell (1881), who provided explicit expressions for the conductivities of some third-rank laminates composed of isotropic constituents. A comprehensive analysis of this complex microstructure was performed by Tartar (1985, 2009), who proved a famous equation giving the permittivity tensor of a two-component rank-m laminate in terms of m arbitrary lamination directions. Similarly, the multiple-rank laminates were also studied from the purely elastic point of view by Francfort and Murat (1986).

More recently, some approaches have been proposed to deal with fully coupled magneto-electro-elastic laminates. Several explicit expressions have been found by Kim (2011) to calculate the magnetic, electric, elastic, piezoelectric, magnetoelastic and magnetoelectric effective properties. On the other hand, similar results have been obtained by Challagulla and Georgiades (2011), Bravo-Castillero, Rodríguez-Ramos, Mechkour, Otero, and Sabina (2008) and Sixto-Camacho et al. (2013) through the asymptotic homogenization and periodic unfolding methods. Since these formalisms have been elaborated for a fixed lamination direction, here we study the general case concerning an arbitrary lamination direction, which is an important point to thoroughly exploit the anisotropic character of the involved components. We develop a self-consistent fully algebraic technique based on the definition of an *ad hoc* operator $\mathcal{P}_{\vec{n}}$, which allows us to explore the effects of the orientation (indicated by $\vec{n}$) of the interfaces on the overall response of the system. The main result is given by a single exact tensor expression furnishing all effective properties of the laminated material. Typically, for developing a homogenization scheme, one needs to consider the differential equation describing the distribution of physical fields. In contrast, we solved the problem by means of the continuity conditions at the interfaces. This alternative approach is justified by the uniformity of the fields induced in each layer. Finally, the definition of tensor $\mathcal{P}_{\vec{n}}$ allows us to further extend our theory in order to consider (i) graded structures with an arbitrary lamination direction and (ii) rank-m laminates with m arbitrary lamination directions. This is a generalization of the Tartar formula to the magneto-electro-elastic coupling. We stress that all the results of the present paper can be also used in the dynamic regime (wave propagation) if we consider a wavelength much larger than the microstructure length scale. In this case, we are working in the so-called quasi-static regime and all components feel a nearly static applied field.

The structure of the paper is the following. In Section 2, we introduce the definitions used to describe linear materials with a coupled behavior. In Section 3, we obtain the response of a single layer and we use this result in Section 4 to develop the theory for the laminated geometry with a fixed lamination direction. In Section 5 we discuss a series of particular cases of the general theory and we present several applications to (artificial or intrinsic) multiferroic materials. Next, we perform the generalization to an arbitrary orientation of interfaces in Section 6. To conclude we introduce graded structures and multiple-rank laminated materials in Sections 7 and 8, respectively.

2. Definitions

In order to take into account all possible couplings among electric, magnetic and elastic quantities, we consider the following generalized relation giving the time variation of the total energy density

$$\frac{du}{dt} = T_{ij}\frac{d\varepsilon_{ij}}{dt} + E_i\frac{dD_i}{dt} + H_i\frac{dB_i}{dt}, \tag{1}$$

where we have supposed an arbitrarily nonlinear energy function $u = u(\hat{\varepsilon}, \vec{D}, \vec{B})$ (Landau, Pitaevskii, & Lifshitz, 1984, 1986). Here T_{ij} represents the Cauchy stress tensor, ε_{ij} the infinitesimal strain tensor, E_i and H_i the electric and magnetic fields and, finally, D_i and B_i the electric and magnetic inductions. From Eq. (1), we immediately obtain the constitutive equations in terms of the energy function

$$T_{ij} = \frac{\partial u(\hat{\varepsilon}, \vec{D}, \vec{B})}{\partial \varepsilon_{ij}}, \quad E_i = \frac{\partial u(\hat{\varepsilon}, \vec{D}, \vec{B})}{\partial D_i} \quad \text{and} \quad H_i = \frac{\partial u(\hat{\varepsilon}, \vec{D}, \vec{B})}{\partial B_i}. \tag{2}$$

In the case of a linear material, we can introduce a tensor relationship

$$\mathcal{K}_0 = \mathcal{L}_0 \mathcal{Z}_0, \tag{3}$$

where we adopted the generalized Voigt notation

$$\mathcal{K}_0^T = (T_{11}, T_{22}, T_{33}, T_{23}, T_{13}, T_{12}, E_1, E_2, E_3, H_1, H_2, H_3), \tag{4}$$

$$\mathcal{Z}_0^T = (\varepsilon_{11}, \varepsilon_{22}, \varepsilon_{33}, 2\varepsilon_{23}, 2\varepsilon_{13}, 2\varepsilon_{12}, D_1, D_2, D_3, B_1, B_2, B_3) \tag{5}$$

and we may prove the symmetry $\mathcal{L}_0 = \mathcal{L}_0^T$ (T means matrix transposition).

In addition, we can adopt an alternative version of the generalized Voigt notation leading to the following linear constitutive equation

$$\mathcal{K} = \mathcal{L}\mathcal{Z}, \tag{6}$$

where

$$\mathcal{K}^T = (T_{11}, T_{22}, T_{33}, T_{23}, T_{13}, T_{12}, D_1, D_2, D_3, B_1, B_2, B_3), \tag{7}$$

$$\mathcal{Z}^T = (\varepsilon_{11}, \varepsilon_{22}, \varepsilon_{33}, 2\varepsilon_{23}, 2\varepsilon_{13}, 2\varepsilon_{12}, -E_1, -E_2, -E_3, -H_1, -H_2, -H_3) \tag{8}$$

and the symmetry $\mathcal{L} = \mathcal{L}^T$ is still preserved. In this work, we use this latter representation where the quantity $\mathcal{L}$ contains the elastic stiffness tensor, the magnetic permeability tensor, the electric permittivity tensor, the piezoelectric tensor, the magnetostrictive tensor and the magnetoelectric tensor. Of course, $\mathcal{L}$ may represent any form of anisotropy, i.e. any kind of crystal symmetry (Nye, 1985; Sirotine & Chaskolskaia, 1984).

3. Single layer formalism

We consider a single layer composed of a linear material $\mathcal{L}_1$ embedded in a homogeneous space $\mathcal{L}_0$. We consider the system remotely loaded by $\mathcal{Z}_0$ and $\mathcal{K}_0$, which are uniform fields generated by remote sources. These fields are those existing in the entire space $\mathcal{L}_0$ before introducing the layer $\mathcal{L}_1$. We suppose that the interfaces are perpendicular to the axis x_3 (see Fig. 1(a) for details). Moreover, we assume that there is no free electric charge and no electric current distributed on the interfaces and we study the continuity of the physical fields across them. As well known, the continuous components of $\mathcal{K}$ across the interface are $T_{13}, T_{23}, T_{33}, D_3$ and B_3. Similarly, the continuous components of $\mathcal{Z}$ are $\varepsilon_{11}, \varepsilon_{12}, \varepsilon_{22}, E_1, E_2, H_1$ and H_2. We observe that these two sets of continuous components are complementary in the structure of vectors $\mathcal{Z}$ and $\mathcal{K}$. It means that the ith component of $\mathcal{Z}$ is continuous if and only if the ith component of $\mathcal{K}$ suffers a discontinuity. This property allows us to build up the following formalism. Since $\mathcal{K}$ and $\mathcal{Z} \in \Re^{12}$ we define a first simple set $\mathbf{C}$ containing the integer numbers from 1 to 12: $\mathbf{C} = \{1, 2, 3, \ldots, 12\}$. Then, we can define $\mathbf{C}_{\mathcal{K}} = \{3, 4, 5, 9, 12\} \subset \mathbf{C}$ as the subset containing the positions of continuous components of $\mathcal{K}$. Of course, we have card $(\mathbf{C}_{\mathcal{K}}) = n$ having defined $n = 5$. Similarly, we can define $\mathbf{C}_{\mathcal{Z}} = \mathbf{C} \setminus \mathbf{C}_{\mathcal{K}} \subset \mathbf{C}$

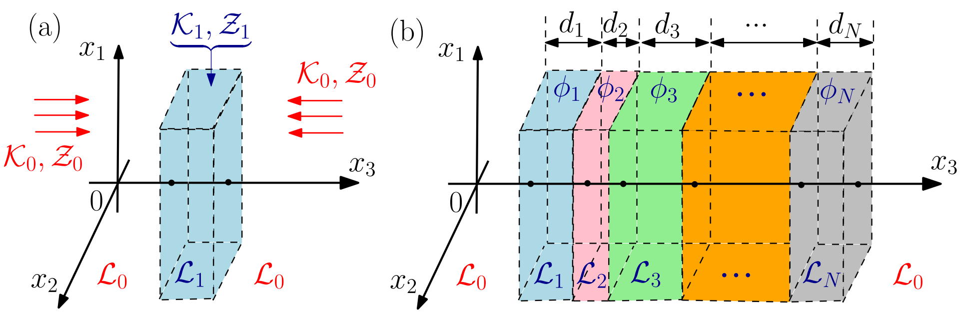

Fig. 1. Schematic representation of a single layer embedded in a homogeneous space (a) and a multilayered structure composed of N different components (b).

as the subset containing the positions of continuous components of $\mathcal{Z}$. As before, we have card $(\mathbf{C}_\mathcal{Z}) = m$ having defined $m = 7$. We introduce now the following matrices

$$\mathcal{P} = \sum_{i=1}^{n}\sum_{j\in\mathbf{C}_\mathcal{K}} \mathcal{F}_{i,j}^{n,n+m} \in \mathbf{M}_{n,n+m}(\Re) \quad \text{and} \quad \mathcal{Q} = \sum_{i=1}^{m}\sum_{j\in\mathbf{C}_\mathcal{Z}} \mathcal{F}_{i,j}^{m,n+m} \in \mathbf{M}_{m,n+m}(\Re), \tag{9}$$

where $\mathcal{F}_{i,j}^{a,b} \in \mathbf{M}_{a,b}(\Re)$ is an elementary matrix with a rows and b columns with the element (i,j) equal to one and all the others equal to zero. The set $\mathbf{M}_{a,b}(\Re)$ represents the linear space of real matrices with a rows and b columns. Moreover, the symbol $\mathcal{I}_r \in \mathbf{M}_{r,r}(\Re)$ represents the identity matrix of order r and $\mathcal{O}_{ab} \in \mathbf{M}_{a,b}(\Re)$ is the null matrix. The following properties hold on

$$\mathcal{P}\mathcal{P}^T = \mathcal{I}_n \quad \text{and} \quad \mathcal{Q}\mathcal{Q}^T = \mathcal{I}_m, \tag{10}$$

$$\mathcal{P}\mathcal{Q}^T = \mathcal{O}_{nm} \quad \text{and} \quad \mathcal{Q}\mathcal{P}^T = \mathcal{O}_{mn}, \tag{11}$$

$$\mathcal{P}^T\mathcal{P} + \mathcal{Q}^T\mathcal{Q} = \mathcal{I}_{n+m}, \tag{12}$$

as one can easily verify. The physical meaning of the matrices $\mathcal{P}$ and $\mathcal{Q}$ becomes evident by considering the following statements. The vector $\mathcal{P}\mathcal{K} \in \Re^n$ contains the continuous components of $\mathcal{K} \in \Re^{n+m}$ across the interface. Similarly, the vector $\mathcal{Q}\mathcal{Z} \in \Re^m$ contains the continuous components of $\mathcal{Z} \in \Re^{n+m}$. Furthermore, other properties will be used in the following developments: the vector $\mathcal{P}^T\mathcal{P}\mathcal{K} \in \Re^{n+m}$ has the same structure as $\mathcal{K}$, but all the discontinuous components are imposed to zero. In other words, we have $(\mathcal{P}^T\mathcal{P}\mathcal{K})_i = \mathcal{K}_i$ if $i \in \mathbf{C}_\mathcal{K}$ and $(\mathcal{P}^T\mathcal{P}\mathcal{K})_i = 0$ if $i \in \mathbf{C}_\mathcal{Z}$. Similarly, $\mathcal{Q}^T\mathcal{Q}\mathcal{Z} \in \Re^{n+m}$ has the same structure as $\mathcal{Z}$, but all the discontinuous components are imposed to zero. It means that $(\mathcal{Q}^T\mathcal{Q}\mathcal{Z})_i = \mathcal{Z}_i$ if $i \in \mathbf{C}_\mathcal{Z}$ and $(\mathcal{Q}^T\mathcal{Q}\mathcal{K})_i = 0$ if $i \in \mathbf{C}_\mathcal{K}$.

We remark that this formalism can be adopted to analyse any linear physical coupling described by two dual sets of variables (here $\mathcal{K}$ and $\mathcal{Z} \in \Re^{n+m}$) exhibiting the continuity of the complementary components (n components of $\mathcal{K}$ and m complementary components of $\mathcal{Z}$) across a given interface. We present here the theory for the magneto-electro-elastic case, but it can be easily generalized to more complex situations, e.g. with thermal and/or other transport properties.

We can now consider a single layer perpendicular to the axis x_3 (Fig. 1(a)). The internal generalized stress $\mathcal{K}_1$ is constituted by the n continuous components of $\mathcal{K}_0$ and by a set of arbitrary components $\mathcal{X} \in \Re^m$. Similarly, the internal generalized strain $\mathcal{Z}_1$ is constituted by the m continuous components of $\mathcal{Z}_0$ and by a set of arbitrary components $\mathcal{Y} \in \Re^n$. Explicitly, we have

$$\mathcal{K}_1 = \mathcal{P}^T\mathcal{P}\mathcal{K}_0 + \mathcal{Q}^T\mathcal{X}, \tag{13}$$

$$\mathcal{Z}_1 = \mathcal{Q}^T\mathcal{Q}\mathcal{Z}_0 + \mathcal{P}^T\mathcal{Y}, \tag{14}$$

with the conditions $\mathcal{K}_1 = \mathcal{L}_1\mathcal{Z}_1$ and $\mathcal{K}_0 = \mathcal{L}_0\mathcal{Z}_0$. We must solve previous equations to find $\mathcal{X} \in \Re^m$ and $\mathcal{Y} \in \Re^n$. By substituting Eqs. (13) and (14) in the constitutive relation of the layer we obtain

$$\mathcal{P}^T\mathcal{P}\mathcal{K}_0 + \mathcal{Q}^T\mathcal{X} = \mathcal{L}_1\mathcal{Q}^T\mathcal{Q}\mathcal{Z}_0 + \mathcal{L}_1\mathcal{P}^T\mathcal{Y}. \tag{15}$$

Now, we apply the operator $\mathcal{P}$ and, by using the properties $\mathcal{P}\mathcal{Q}^T = 0$ and $\mathcal{P}\mathcal{P}^T = \mathcal{I}_n$, we easily obtain the vector $\mathcal{Y}$

$$\mathcal{Y} = \left(\mathcal{P}\mathcal{L}_1\mathcal{P}^T\right)^{-1}\left(\mathcal{P}\mathcal{K}_0 - \mathcal{P}\mathcal{L}_1\mathcal{Q}^T\mathcal{Q}\mathcal{Z}_0\right). \tag{16}$$

The resulting expression for $\mathcal{Z}_1$ follows

$$\mathcal{Z}_1 = \left[\mathcal{Q}^T\mathcal{Q} + \mathcal{P}^T\left(\mathcal{P}\mathcal{L}_1\mathcal{P}^T\right)^{-1}\mathcal{P}\left(\mathcal{L}_0 - \mathcal{L}_1\mathcal{Q}^T\mathcal{Q}\right)\right]\mathcal{Z}_0. \tag{17}$$

Finally, by using the property $\mathcal{P}^T\mathcal{P} + \mathcal{Q}^T\mathcal{Q} = \mathcal{I}_{n+m}$, Eq. (17) can be elaborated, eventually obtaining

$$\mathcal{Z}_1 = \left[\mathcal{I}_{n+m} + \mathcal{P}^T\left(\mathcal{P}\mathcal{L}_1\mathcal{P}^T\right)^{-1}\mathcal{P}\left(\mathcal{L}_0 - \mathcal{L}_1\right)\right]\mathcal{Z}_0. \tag{18}$$

Of course, the generalized stress can be directly calculated through the relation $\mathcal{K}_1 = \mathcal{L}_1\mathcal{Z}_1$. We have therefore obtained the solutions giving the internal physical fields when the externally applied ones are known. Interestingly enough, these results are independent of the layer thickness. We also note that only a single auxiliary matrix $\mathcal{P}$ is sufficient to write the internal fields in closed form (i.e. $\mathcal{Q}$ is not necessary in final equations). As expected, the physical fields are uniform in the whole space (i.e. $\mathcal{K}_1 = \mathcal{K}_0$ and $\mathcal{Z}_1 = \mathcal{Z}_0$) if $\mathcal{L}_0 = \mathcal{L}_1$. The usefulness of the lamination operator $\mathcal{P}$ will be even more evident when we consider an arbitrary lamination direction.

4. Homogenization for a fixed lamination direction

We consider now a laminated structure composed of N different layers, each described by a tensor $\mathcal{L}_i$ and having a thickness $d_i, i = 1, \ldots, N$ (Fig. 1(b)). We can define the volume fraction of each component as $\phi_i = d_i/D$ where $D = \sum_{i=1}^{N} d_i$ is the total length of the heterostructure. As before, the external material is described by $\mathcal{L}_0$ and the system is loaded by remotely applied uniform fields $\mathcal{Z}_0$ and $\mathcal{K}_0 = \mathcal{L}_0\mathcal{Z}_0$. All interfaces are perpendicular to axis x_3. Because of the geometry of the system, the determination of the internal fields performed in the previous Section is valid for each layer of the present composite structure. Therefore, the local generalized stress $\mathcal{K}_i$ and the local generalized strains $\mathcal{Z}_i$ are given by

$$\mathcal{K}_i = \mathcal{L}_i\mathcal{A}_i\mathcal{Z}_0 \quad \text{and} \quad \mathcal{Z}_i = \mathcal{A}_i\mathcal{Z}_0 \tag{19}$$

for any $i = 1, \ldots, N$, where $\mathcal{A}_i$ represents the layer concentration tensor (see Eq. (18)) given by

$$\mathcal{A}_i = \mathcal{I}_{n+m} + \mathcal{P}^T\left(\mathcal{P}\mathcal{L}_i\mathcal{P}^T\right)^{-1}\mathcal{P}(\mathcal{L}_0 - \mathcal{L}_i). \tag{20}$$

In order to obtain the effective response of the multilayered structure we evaluate the average value of the physical fields over the whole system

$$\langle\mathcal{K}\rangle = \sum_{i=1}^{N}\phi_i\mathcal{K}_i = \left(\sum_{i=1}^{N}\phi_i\mathcal{L}_i\mathcal{A}_i\right)\mathcal{Z}_0, \tag{21}$$

$$\langle\mathcal{Z}\rangle = \sum_{i=1}^{N}\phi_i\mathcal{Z}_i = \left(\sum_{i=1}^{N}\phi_i\mathcal{A}_i\right)\mathcal{Z}_0. \tag{22}$$

By determining $\mathcal{Z}_0$ from Eq. (22) and substituting the result in Eq. (21) we obtain the effective tensor of the structure defined through the relation $\langle\mathcal{K}\rangle = \mathcal{L}_{eff}\langle\mathcal{Z}\rangle$; we simply have

$$\mathcal{L}_{eff} = \left(\sum_{i=1}^{N}\phi_i\mathcal{L}_i\mathcal{A}_i\right)\left(\sum_{i=1}^{N}\phi_i\mathcal{A}_i\right)^{-1}, \tag{23}$$

or, more explicitly using Eq. (21)

$$\mathcal{L}_{eff} = \left[\sum_{i=1}^{N}\phi_i\mathcal{L}_i + \sum_{i=1}^{N}\phi_i\mathcal{L}_i\mathcal{P}^T\left(\mathcal{P}\mathcal{L}_i\mathcal{P}^T\right)^{-1}\mathcal{P}(\mathcal{L}_0 - \mathcal{L}_i)\right] \times \left[\mathcal{I}_{n+m} + \sum_{i=1}^{N}\phi_i\mathcal{P}^T\left(\mathcal{P}\mathcal{L}_i\mathcal{P}^T\right)^{-1}\mathcal{P}(\mathcal{L}_0 - \mathcal{L}_i)\right]^{-1}. \tag{24}$$

The last expression represents the effective tensor of the laminated material. However, in order to prove the coherence of this result, we must show that $\mathcal{L}_{eff}$ does not depend on tensor $\mathcal{L}_0$ describing the behavior of the external medium. As a matter of fact, we demonstrate that the effective tensor $\mathcal{L}_{eff}$ depends only on the components tensors $\mathcal{L}_i$ and on the stoichiometric coefficients ϕ_i with $i = 1, \ldots, N$. The proposed proof consists in obtaining a new form of Eq. (24) where $\mathcal{L}_0$ is not present. To this aim, we introduce a theorem valid for any matrix $\mathcal{S} \in \mathbf{M}_{n+m,n}(\Re)$ and $\mathcal{R} \in \mathbf{M}_{n,n+m}(\Re)$ such that $(\mathcal{I}_{n+m} + \mathcal{S}\mathcal{R})$ and $(\mathcal{I}_{n+m} + \mathcal{R}\mathcal{S})$ are not singular

$$(\mathcal{I}_{n+m} + \mathcal{S}\mathcal{R})^{-1} = \mathcal{I}_{n+m} - \mathcal{S}(\mathcal{I}_{n+m} + \mathcal{R}\mathcal{S})^{-1}\mathcal{R}. \tag{25}$$

It can be easily proved by considering $\left[\mathcal{I}_{n+m} - \mathcal{S}(\mathcal{I}_{n+m} + \mathcal{R}\mathcal{S})^{-1}\mathcal{R}\right](\mathcal{I}_{n+m} + \mathcal{S}\mathcal{R})$, by using the relation $\mathcal{R}\mathcal{I}_{n+m} = \mathcal{I}_n\mathcal{R}$ and by obtaining the result $\mathcal{I}_{n+m}$, as requested. We can now use this property for elaborating the inverse matrix appearing in the second line of Eq. (24) by letting $\mathcal{S} = \mathcal{P}^T$ and $\mathcal{R} = \sum_{i=1}^{N}\phi_i\left(\mathcal{P}\mathcal{L}_i\mathcal{P}^T\right)^{-1}\mathcal{P}(\mathcal{L}_0 - \mathcal{L}_i)$. So doing, the term $\mathcal{I}_{n+m} + \mathcal{R}\mathcal{S}$ in the right hand side of Eq. (25) reads $\mathcal{I}_{n+m} + \mathcal{R}\mathcal{S} = \sum_{i=1}^{N}\phi_i\left(\mathcal{P}\mathcal{L}_i\mathcal{P}^T\right)^{-1}\mathcal{P}\mathcal{L}_0\mathcal{P}^T$, where we used the condition $\sum_{i=1}^{N}\phi_i = 1$. Hence, the effective tensor assumes the following form

$$\begin{aligned}
\mathcal{L}_{eff} = &\sum_{i=1}^{N}\phi_i\mathcal{L}_i + \sum_{i=1}^{N}\phi_i\mathcal{L}_i\mathcal{P}^T\left(\mathcal{P}\mathcal{L}_i\mathcal{P}^T\right)^{-1}\mathcal{P}(\mathcal{L}_0 - \mathcal{L}_i) \\
&- \sum_{k=1}^{N}\phi_k\mathcal{L}_k\mathcal{P}^T\left(\mathcal{P}\mathcal{L}_0\mathcal{P}^T\right)^{-1}\left[\sum_{i=1}^{N}\phi_i\left(\mathcal{P}\mathcal{L}_i\mathcal{P}^T\right)^{-1}\right]^{-1}\sum_{j=1}^{N}\phi_j\left(\mathcal{P}\mathcal{L}_j\mathcal{P}^T\right)^{-1}\mathcal{P}(\mathcal{L}_0 - \mathcal{L}_j) \\
&- \sum_{k=1}^{N}\phi_k\mathcal{L}_k\mathcal{P}^T\left(\mathcal{P}\mathcal{L}_k\mathcal{P}^T\right)^{-1}\mathcal{P}(\mathcal{L}_0 - \mathcal{L}_k)\mathcal{P}^T\left(\mathcal{P}\mathcal{L}_0\mathcal{P}^T\right)^{-1}\left[\sum_{i=1}^{N}\phi_i\left(\mathcal{P}\mathcal{L}_i\mathcal{P}^T\right)^{-1}\right]^{-1}\sum_{j=1}^{N}\phi_j\left(\mathcal{P}\mathcal{L}_j\mathcal{P}^T\right)^{-1}\mathcal{P}(\mathcal{L}_0 - \mathcal{L}_j).
\end{aligned} \tag{26}$$

Now, we can expand the terms $\mathcal{L}_0 - \mathcal{L}_i, \mathcal{L}_0 - \mathcal{L}_j$ and $\mathcal{L}_0 - \mathcal{L}_k$ and, after a very long but straightforward calculation, we can prove that all terms containing $\mathcal{L}_0$ disappear. We eventually find the final result

$$\mathcal{L}_{eff} = \sum_{i=1}^{N}\phi_i\mathcal{L}_i - \sum_{i=1}^{N}\phi_i\mathcal{L}_i\mathcal{P}^T\left(\mathcal{P}\mathcal{L}_i\mathcal{P}^T\right)^{-1}\mathcal{P}\mathcal{L}_i + \sum_{k=1}^{N}\phi_k\mathcal{L}_k\mathcal{P}^T\left(\mathcal{P}\mathcal{L}_k\mathcal{P}^T\right)^{-1}\left[\sum_{i=1}^{N}\phi_i\left(\mathcal{P}\mathcal{L}_i\mathcal{P}^T\right)^{-1}\right]^{-1}\sum_{j=1}^{N}\phi_j\left(\mathcal{P}\mathcal{L}_j\mathcal{P}^T\right)^{-1}\mathcal{P}\mathcal{L}_j, \tag{27}$$

where the matrix $\mathcal{P}$ defined in Eq. (9) can be given explicitly as

$$\mathcal{P} = \begin{pmatrix} 0 & 0 & 1 & 0 & 0 & 0 & 0 & 0 & 0 & 0 & 0 & 0 \\ 0 & 0 & 0 & 1 & 0 & 0 & 0 & 0 & 0 & 0 & 0 & 0 \\ 0 & 0 & 0 & 0 & 1 & 0 & 0 & 0 & 0 & 0 & 0 & 0 \\ 0 & 0 & 0 & 0 & 0 & 0 & 0 & 0 & 1 & 0 & 0 & 0 \\ 0 & 0 & 0 & 0 & 0 & 0 & 0 & 0 & 0 & 0 & 0 & 1 \end{pmatrix}. \tag{28}$$

Eq. (27) is the main result of the present Section: it represents a closed-form expression of the effective tensor of the structure. We briefly summarize here the practical application of Eq. (27): each layer is characterized by tensor $\mathcal{L}_i$ (describing all the physical properties and their couplings, as defined in Section 2) and by volume fraction ϕ_i, which is simply proportional to the thickness of the layer (with $\sum_{i=1}^{N}\phi_i = 1$). The tensor $\mathcal{P}$ given in Eq. (28) indicates that the lamination direction corresponds to x_3. Below, we will prove that Eq. (27) remains valid when we consider an arbitrary lamination direction $\vec{n}$, provided that we use the operator $\mathcal{P}_{\vec{n}}$ defined in Eq. (65) in place of $\mathcal{P}$ (see Section 6 for details). The result obtained through Eq. (27) represents the overall average response of the multilayer system. Therefore, we can write $\mathcal{L}_{eff} = \mathcal{L}_{eff}(\mathcal{L}_1,\ldots,\mathcal{L}_N;\phi_1,\ldots,\phi_N)$, for a given lamination tensor $\mathcal{P}$ (or $\mathcal{P}_{\vec{n}}$). Interestingly enough, a single matrix expression provides all the effective coupling properties of the whole structure. This points is very convenient from the computational point of view. We underline in fact that Eq. (27) can be simply implemented in a software code through the basic operations of matrix algebra. In particular, we need to calculate $N+1$ inverse matrices, where N is the number of layers. The result in Eq. (27) fulfils a series of rules with a simple physical meaning:

- *homogeneity*: it means that we can rescale the units of measurement without loosing the structure of the formula

$$\mathcal{L}_{eff}(\lambda\mathcal{L}_1,\ldots,\lambda\mathcal{L}_N;\phi_1,\ldots,\phi_N) = \lambda\mathcal{L}_{eff}(\mathcal{L}_1,\ldots,\mathcal{L}_N;\phi_1,\ldots,\phi_N) \quad \forall\lambda\in\Re; \tag{29}$$

- *boundary conditions*: when only one component is present we must have the effective tensor properties coinciding with its specific tensor

$$\mathcal{L}_{eff}(\mathcal{L}_1,\ldots,\mathcal{L}_N;\phi_j = 0\forall j\neq i,\phi_i = 1) = \mathcal{L}_i \quad \forall i = 1,\ldots,N; \tag{30}$$

- *undistinguishability*: for a two-phase laminated material the components are undistinguishable (it is also true for the N-phase structure if we apply an arbitrary permutation of constituents)

$$\mathcal{L}_{eff}(\mathcal{L}_1,\mathcal{L}_2;\phi_1,\phi_2) = \mathcal{L}_{eff}(\mathcal{L}_2,\mathcal{L}_1;\phi_2,\phi_1); \tag{31}$$

- *two-step calculability*: if we deal with a three-phase system we can determine the effective response either directly with the expression for three components or by using iteratively (twice) the expression for two components

$$\mathcal{L}_{eff}(\mathcal{L}_1,\mathcal{L}_2,\mathcal{L}_3;\phi_1,\phi_2,\phi_3) = \mathcal{L}_{eff}\left(\mathcal{L}_{eff}\left(\mathcal{L}_1,\mathcal{L}_2;\frac{\phi_1}{\phi_1+\phi_2},\frac{\phi_2}{\phi_1+\phi_2}\right),\mathcal{L}_3;\phi_1+\phi_2,\phi_3\right). \tag{32}$$

Of course, the final tensor $\mathcal{L}_{eff}$ exhibits the standard symmetry $\mathcal{L}_{eff} = \mathcal{L}_{eff}^T$.

5. Analysis of uncoupled cases and some examples of application

In order to show the applicability of the general theory to realistic problems, we present in this Section the analysis of simple specific cases (uncoupled systems) and we use the general formalism for some more advanced multiferroic structures. The following situations will be considered:

1. linear analysis of purely electric (or magnetic) isotropic systems: we prove that the classical results reported in the literature (Milton, 2004; Tartar, 1979) can be obtained as a particular case of our general formalism;
2. linear analysis of purely elastic isotropic systems: again, we obtain the classical results for the linear response (Backus, 1962; Postma, 1955; Milton, 2004) as specific cases of our theory;
3. analysis of artificial multiferroics: we apply the general solution to numerically determine the magnetoelectric response of piezoelectric/magnetoelastic laminates. We will stress the good agreement with some results published in recent papers;
4. analysis of more realistic artificial multiferroics with a pure elastic interphase between the piezoelectric and magnetoelastic layers. We will study the degradation of the magnetoelectric response in terms of interphase properties;
5. linear properties of coupled magnetoelectric isotropic systems: we perform a theoretical analysis providing the complete effective constitutive equation of a laminated system composed of different magnetoelectric layers (intrinsic multiferroics).

5.1. Analysis of purely dielectric multilayers

We consider the particular case corresponding to the homogenization of purely dielectric structures. To begin, we suppose to deal with a sequence of anisotropic layers having permittivity tensors $\hat{\epsilon}_i$, volume fractions ϕ_i and an effective permittivity tensor $\hat{\epsilon}_{eff}$ (the lamination direction is x_3 as before). It is simple to prove that Eq. (27) reduces to the following simpler version

$$\hat{\epsilon}_{eff} = \sum_{i=1}^{N}\phi_i\hat{\epsilon}_i - \sum_{i=1}^{N}\phi_i\frac{(\hat{\epsilon}_i\vec{e}_3)\otimes(\hat{\epsilon}_i\vec{e}_3)}{\vec{e}_3\cdot\hat{\epsilon}_i\vec{e}_3} + \sum_{k=1}^{N}\sum_{j=1}^{N}\phi_k\phi_j\frac{(\hat{\epsilon}_k\vec{e}_3)\otimes(\hat{\epsilon}_j\vec{e}_3)}{(\vec{e}_3\cdot\hat{\epsilon}_k\vec{e}_3)(\vec{e}_3\cdot\hat{\epsilon}_j\vec{e}_3)}\frac{1}{\sum_{i=1}^{N}\frac{\phi_i}{\vec{e}_3\cdot\hat{\epsilon}_i\vec{e}_3}} \tag{33}$$

where $\vec{e}_i$ is the unit vector in direction x_i, $\hat{\epsilon}_i\vec{v}$ represents the standard matrix–vector product (here $\vec{v}$ is an arbitrary vector) and, finally, $\widehat{A} = \vec{b}\otimes\vec{c}$ represents the tensor product, i.e. $A_{ij} = b_i c_j$. In order to explicitly prove Eq. (33), one can entirely repeat, step by step, the whole proof given in Section 4, considering only the terms related to the electric permittivity. Alternatively, it is simple to observe that Eq. (33) is formally identical to Eq. (27) provided that we substitute operator $\mathcal{P}$ with the scalar product with the unit vector $\vec{e}_3$, representing the actual lamination direction. Moreover, according to the analysis performed in Section 6, we also remark that Eq. (33) remains valid for an arbitrary lamination direction if we substitute $\vec{e}_3$ with a given unit vector $\vec{n}$. Interestingly enough, we underline that the result given in Eq. (33) (or the version with an arbitrary $\vec{n}$ in place of $\vec{e}_3$) can be equally applied to homogenize other physical properties such as the magnetic permeability tensor, the electric or thermal conductivity tensor and the diffusion tensor in a given transport process. Although Eq. (33) is an explicit result of direct applicability for homogenizing arbitrarily anisotropic structures, it is interesting to study the case with isotropic layers described by $\hat{\epsilon}_i = \epsilon_i\widehat{I}$ (where ϵ_i is the scalar permittivity and $\widehat{I}$ is the 3×3 identity matrix). In this case we can simplify Eq. (33), as follows

$$\hat{\epsilon}_{eff} = \sum_{i=1}^{N}\phi_i\epsilon_i\widehat{I} - \sum_{i=1}^{N}\phi_i\frac{\epsilon_i^2\vec{e}_3\otimes\vec{e}_3}{\epsilon_i} + \sum_{k=1}^{N}\sum_{j=1}^{N}\phi_k\phi_j\frac{\epsilon_k\epsilon_j\vec{e}_3\otimes\vec{e}_3}{\epsilon_k\epsilon_j}\frac{1}{\sum_{i=1}^{N}\frac{\phi_i}{\epsilon_i}}. \tag{34}$$

Since $\sum_{k=1}^{N}\phi_k = 1$ we further obtain

$$\hat{\epsilon}_{eff} = \sum_{i=1}^{N}\phi_i\epsilon_i\widehat{I} - \sum_{i=1}^{N}\phi_i\epsilon_i\vec{e}_3\otimes\vec{e}_3 + \frac{1}{\sum_{i=1}^{N}\frac{\phi_i}{\epsilon_i}}\vec{e}_3\otimes\vec{e}_3, \tag{35}$$

or, recalling that $\widehat{I} = \vec{e}_1\otimes\vec{e}_1 + \vec{e}_2\otimes\vec{e}_2 + \vec{e}_3\otimes\vec{e}_3$, we have

$$\hat{\epsilon}_{eff} = \sum_{i=1}^{N}\phi_i\epsilon_i(\vec{e}_1\otimes\vec{e}_1 + \vec{e}_2\otimes\vec{e}_2) + \frac{1}{\sum_{i=1}^{N}\frac{\phi_i}{\epsilon_i}}\vec{e}_3\otimes\vec{e}_3. \tag{36}$$

Now, it is easy to identify the longitudinal ($\|$) and the transverse ($\perp$) components of the effective permittivity tensor, defined through $\hat{\epsilon}_{eff} = \epsilon_{eff,\perp}(\vec{e}_1\otimes\vec{e}_1 + \vec{e}_2\otimes\vec{e}_2) + \epsilon_{eff,\|}\,\vec{e}_3\otimes\vec{e}_3$; we have

$$\epsilon_{eff,\perp} = \sum_{i=1}^{N}\phi_i\epsilon_i = \langle\epsilon\rangle \quad \text{and} \quad \epsilon_{eff,\|} = \frac{1}{\sum_{i=1}^{N}\frac{\phi_i}{\epsilon_i}} = \frac{1}{\left\langle\frac{1}{\epsilon}\right\rangle}, \tag{37}$$

which are the classical results for the dielectric constant of layers connected in parallel and in series, respectively. Here $\langle z\rangle = \sum_{i=1}^{N}\phi_i z_i$ is the weighted arithmetic mean over the sequence of layers. Of course, the same analysis can be simply conducted with an arbitrary unit vector $\vec{n}$ in place of $\vec{e}_3$. In the light of this result, we can say that our general solution given in Eq. (33) (or Eq. (27)) is a tensor generalization of the standard rules for determining the equivalent behavior of components connected in series (longitudinal direction) and in parallel (transverse direction).

5.2. Analysis of purely elastic multilayers

In this section we analyse the mechanical behavior of multilayered structures. Since we are dealing with a pure elastic system, we can adopt the following simplified quantities

$$\mathcal{T} = (T_{11}, T_{22}, T_{33}, T_{23}, T_{13}, T_{12})^T, \quad \mathcal{E} = (\varepsilon_{11}, \varepsilon_{22}, \varepsilon_{33}, 2\varepsilon_{23}, 2\varepsilon_{13}, 2\varepsilon_{12})^T, \tag{38}$$

leading to the constitutive equations $\mathcal{T} = \mathcal{C}_i\mathcal{E}$ in each layer (the 6×6 matrix $\mathcal{C}_i$ contains all the elastic constants of the materials). The general analysis conducted in the previous Section remains valid with minor modifications: the effective elastic tensor is in fact given by the following expression

$$\mathcal{C}_{eff} = \sum_{i=1}^{N}\phi_i\mathcal{C}_i - \sum_{i=1}^{N}\phi_i\mathcal{C}_i\mathcal{P}_e^T\left(\mathcal{P}_e\mathcal{C}_i\mathcal{P}_e^T\right)^{-1}\mathcal{P}_e\mathcal{C}_i + \sum_{k=1}^{N}\phi_k\mathcal{C}_k\mathcal{P}_e^T\left(\mathcal{P}_e\mathcal{C}_k\mathcal{P}_e^T\right)^{-1}\left[\sum_{i=1}^{N}\phi_i\left(\mathcal{P}_e\mathcal{C}_i\mathcal{P}_e^T\right)^{-1}\right]^{-1}\sum_{j=1}^{N}\phi_j\left(\mathcal{P}_e\mathcal{C}_j\mathcal{P}_e^T\right)^{-1}\mathcal{P}_e\mathcal{C}_j, \tag{39}$$

where the elastic version $\mathcal{P}_e$ of the lamination tensor (along the axis x_3) assumes the simpler form

$$\mathcal{P}_e = \begin{pmatrix} 0 & 0 & 1 & 0 & 0 & 0 \\ 0 & 0 & 0 & 1 & 0 & 0 \\ 0 & 0 & 0 & 0 & 1 & 0 \end{pmatrix}. \tag{40}$$

This result can be easily implemented in order to study laminated materials with an arbitrary elastic anisotropy. Nevertheless, it is interesting to analyse specific results concerning isotropic structures. We introduce the constitutive equation for an isotropic linear elastic material, which is valid in each layer ($i = 1\ldots N$)

$$T_{kh} = 2\mu_i\varepsilon_{kh} + \lambda_i\varepsilon_{qq}\delta_{kh}, \tag{41}$$

where λ_i and μ_i are the standard Lamé coefficients of the ith layer, T_{kh} the components of the stress, ε_{kh} the components of the strain and $\varepsilon_{qq} = \mathrm{Tr}(\hat{\varepsilon})$. It means that now $\mathcal{T} = \mathcal{C}_i(\lambda_i, \mu_i)\mathcal{E}$, where the structure of $\mathcal{C}_i(\lambda_i, \mu_i)$ is standard within the context of the

Voigt notation. After a long but straightforward application of Eq. (39), we can obtain the effective elastic properties of the multilayered structure in the form

$$\mathcal{T} = \mathcal{C}_{eff}\,\mathcal{E} = \begin{pmatrix} k+m & k-m & l & 0 & 0 & 0 \\ k-m & k+m & l & 0 & 0 & 0 \\ l & l & n & 0 & 0 & 0 \\ 0 & 0 & 0 & m & 0 & 0 \\ 0 & 0 & 0 & 0 & p & 0 \\ 0 & 0 & 0 & 0 & 0 & p \end{pmatrix} \mathcal{E}. \tag{42}$$

The resulting transversely isotropic material is described by the so called Hill parameters defined as follows

$$k = \sum_{i=1}^{N} \frac{\phi_i \mu_i (2\mu_i + 3\lambda_i)}{2\mu_i + \lambda_i} + \left(\sum_{i=1}^{N} \frac{\phi_i \lambda_i}{2\mu_i + \lambda_i}\right)^2 \left(\sum_{i=1}^{N} \frac{\phi_i}{2\mu_i + \lambda_i}\right)^{-1} = \left\langle \frac{\mu(2\mu + 3\lambda)}{2\mu + \lambda} \right\rangle + \left\langle \frac{\lambda}{2\mu + \lambda} \right\rangle^2 \left\langle \frac{1}{2\mu + \lambda} \right\rangle^{-1}, \tag{43}$$

$$m = \sum_{i=1}^{N} \phi_i \mu_i = \langle \mu \rangle, \tag{44}$$

$$l = \left(\sum_{i=1}^{N} \frac{\phi_i \lambda_i}{2\mu_i + \lambda_i}\right) \left(\sum_{i=1}^{N} \frac{\phi_i}{2\mu_i + \lambda_i}\right)^{-1} = \left\langle \frac{\lambda}{2\mu + \lambda} \right\rangle \left\langle \frac{1}{2\mu + \lambda} \right\rangle^{-1}, \tag{45}$$

$$n = \left(\sum_{i=1}^{N} \frac{\phi_i}{2\mu_i + \lambda_i}\right)^{-1} = \left\langle \frac{1}{2\mu + \lambda} \right\rangle^{-1}, \tag{46}$$

$$p = \left(\sum_{i=1}^{N} \frac{\phi_i}{\mu_i}\right)^{-1} = \left\langle \frac{1}{\mu} \right\rangle^{-1}. \tag{47}$$

These results are in perfect agreement with classical findings of Postma (1955) and Backus (1962); see also Milton (2004) for further details. They can be used to determine the velocities of elastic waves propagating in stratified media under the long wavelength assumption; this point plays a central role in several geophysics investigations.

5.3. Analysis of piezoelectric/magnetoelastic systems

We consider here the simplest configurations of multilayers composed of piezoelectric (PE) and magnetoelastic (ME) phases. In particular, we utilize the PE ceramic $BaTiO_3$ and the ME ferrite $CoFe_2O_4$, whose physical properties are reported in Appendix A. Both materials exhibit a transversely isotropic symmetry (corresponding to an uniaxial behavior) and therefore their crystal orientation can be defined through a given poling direction, as indicated in Fig. 2. We consider the four geometries obtained with parallel and orthogonal alignment of the poling directions of the two components. We present here the results concerning the magneto-electric properties. It is indeed interesting to observe the emergence of the magneto-electric response generated by the combination of piezoelectric and magnetoelastic properties of two materials that have no intrinsic magneto-electric coupling. The result is given by tensor $\mathbf{G} = \{g_{ij}\}$, in general non symmetric, describing the relation $\vec{D} = \mathbf{G}\vec{H}$ (with $\hat{\varepsilon} = 0$ and $\vec{E} = 0$) or, equivalently, $\vec{B} = \mathbf{G}^T\vec{E}$ (with $\hat{\varepsilon} = 0$ and $\vec{H} = 0$). The form of these two relations is simply obtained through the general symmetry of matrix $\mathcal{L}$, introduced in Section 2. In Fig. 2, the components g_{ij} are represented in terms of volume fraction c of the PE phase. Of course, we always have $g_{ij} = 0$ if $c = 0$ (pure ME response) or $c = 1$ (pure PE response). The first case (Fig. 2(a)) is the only one described by an effective behavior corresponding to a transversely isotropic symmetry, similarly to the single phases composing the system. From a quantitative point of view, we observe that the largest magneto-electric response is obtained in the first system where $g_{11} = g_{22} \cong -3.5 \times 10^{-8}$s/m for $c = 1/2$, while g_{33} is quite negligible. In the second structure (Fig. 2(b)), we find a component g_{11} ten times lower than the previous value. We also note that, in the third case (Fig. 2(c)), we have $|g_{13}| > |g_{31}|$, while in the fourth one (Fig. 2(d)), we obtained $|g_{13}| < |g_{31}|$. We underline that the results corresponding to Fig. 2(a) are in perfect agreement with those reported by Kim (2011). In Figs. 3 and 4, we studied more complex structures realized by rotating the poling axis of some layers. Drawing a comparison with the case of Fig. 2(a), we observe that the main contribution to the magneto-electric response is always generated by the layers with the poling directions aligned with the x_3-axis (lamination direction) and is always measured by the $\mathbf{G}$ components g_{11} and g_{22}. More refined effects related to the lamination orientation are discussed in Section 6.

5.4. Analysis of artificial multiferroics with elastic interphases

We consider a configuration involving piezoelectric (PE) and magnetoelastic (ME) phases with a purely elastic interphase. This corresponds to realistic situation where PE and ME materials are assembled with a glue layer. We utilize, as before, the PE ceramic $BaTiO_3$ and the ME compound $CoFe_2O_4$. For simplicity, we consider here the case with both the poling directions aligned to the lamination axis x_3. We suppose to have a purely elastic isotropic layer (EL) between the PE and the ME ones. It

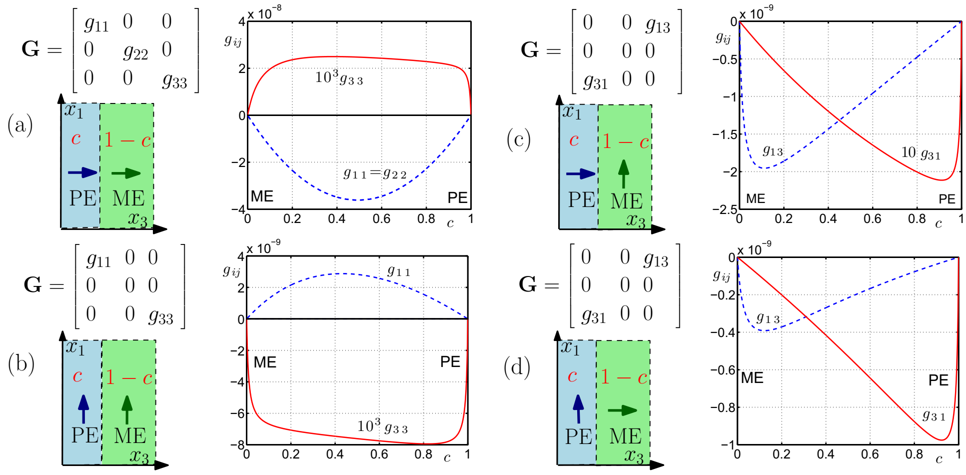

Fig. 2. Magneto-electric response of simple combinations of piezoelectric (PE) and magnetoelastic (ME) layers. We considered four cases representing the parallel and orthogonal configurations of the poling directions. For each case we represented only the magnetoelectric components different from zero as function of the volume fraction c of the PE material.

has a shear modulus $\mu_{in} = 40 \times 10^9$ Pa and a Poisson ratio $\nu_{in} = 0.37$. The volume fractions are defined as follows: $\phi_{PE} = cx$, $\phi_{ME} = x(1-c)$ and $\phi_{EL} = 1 - x$, where the stoichiometric coefficients c and x vary in the range (0,1).

In Fig. 5, the components g_{ij} are represented in terms of x and c. We can observe the absence of magneto-electric effect for $x = 0$ (pure elastic system EL) and the strongest magneto-electric effect for $x = 1$ (absence of elastic interphase between ME and PE subsystems). Moreover, we always have $g_{ij} = 0$ if $c = 0$ (pure ME response) or $c = 1$ (pure PE response). Note that we have represented g_{33} in logarithmic scale because of its very small values. The results for $x = 1$ are in perfect agreement with the first case discussed in the previous example (see Fig. 2(a)). We observe in fact that the largest magneto-electric response $g_{11} = g_{22} \cong -3.5 \times 10^{-8}$ s/m is obtained for $x = 1$ and $c = 1/2$ (however, g_{33} is quite negligible).

In Fig. 6, we investigated the effects of the elastic properties of the interphase on the overall magneto-electric behavior of the system. We considered an elastic layer with a fixed Poisson ratio $\nu_{in} = 0.37$, but with a variable shear modulus μ_{in} in the range $10^6 - 10^{12}$ Pa. In Fig. 6(a), we show $g_{11} = g_{22}$ versus x and $\log_{10}\mu_{in}$ for $c = 1/2$; similarly, in Fig. 6(b), the same quantity is shown versus c and $\log_{10}\mu_{in}$ for $x = 1/2$. We observe that for small values of μ_{in}, we obtain a very weak magneto-electric interaction since the elastic layer is too soft to transmit the needed mechanical stress. On the other hand, for higher values of μ_{in}, we find a stronger magneto-electric coupling caused by a more intense elastic interaction. In the limiting case of a completely rigid interphase, we do not observe any degradation of the effective magneto-electric response.

5.5. Analysis of magnetoelectric multilayers

We introduce a simple isotropic magneto-electric laminated system (along x_3) where each layer is described by the following constitutive equations

$$\vec{D} = \epsilon_i \vec{E} + g_i \vec{H} \tag{48}$$

$$\vec{B} = g_i \vec{E} + \mu_i \vec{H}. \tag{49}$$

It means that each layer ($i = 1 \ldots N$) is made of an intrinsic multiferroic where there is a direct coupling between the magnetic and the electric response. In such a case, the coupling is intrinsic to the material and not mediated by any mechanical

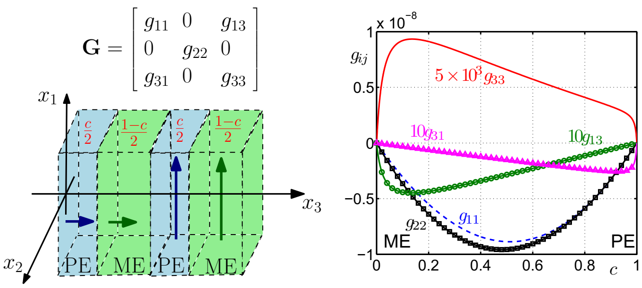

Fig. 3. Magnetoelectric response of a PE–ME four-layer structure.

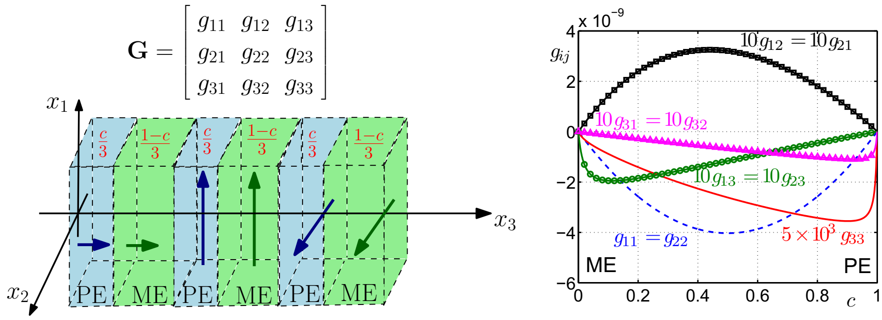

Fig. 4. Magnetoelectric response of a PE–ME six-layer structure.

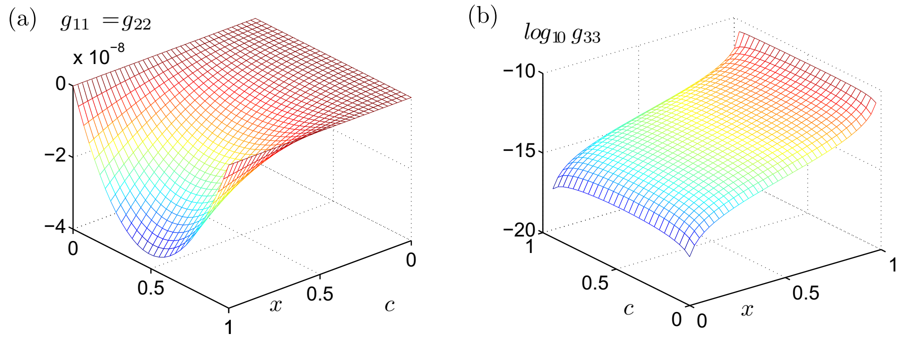

Fig. 5. Magneto-electric response of the combination PE/EL/ME: (a) $g_{11} = g_{22}$ is shown versus x and c, (b) similarly, g_{33} is shown versus x and c. In both cases we used an elastic interphase with a shear modulus $\mu_{in} = 40 \times 10^9$Pa and a Poisson ratio $\nu_{in} = 0.37$.

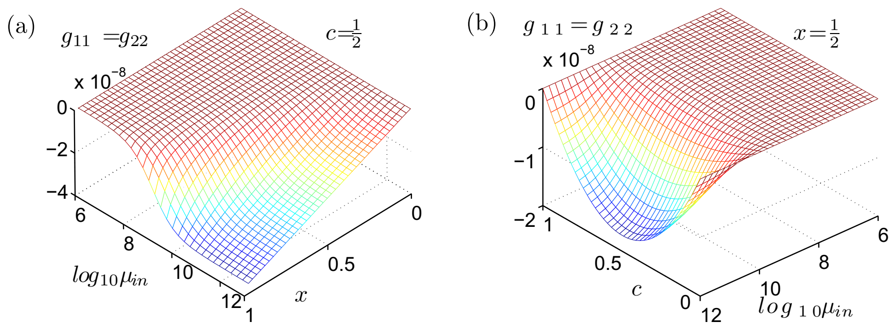

Fig. 6. Magneto-electric response of the combination PE/EL/ME: (a) $g_{11} = g_{22}$ is shown versus x and $\log_{10}\mu_{in}$ for $c = 1/2$, (b) similarly, $g_{11} = g_{22}$ is shown versus c and $\log_{10}\mu_{in}$ for $x = 1/2$. In both cases we used an elastic intephase with a Poisson ratio $\nu_{in} = 0.37$.

interaction. This kind of material is a so-called Tellegen medium where ϵ_i, μ_i and g_i are real parameters; see Sihvola (1994) for further details.

In order to apply the homogenization procedure, we can adopt the general solution given in Eq. (27) by neglecting the elastic components. For the sake of brevity, we omit here the technical development, which is very similar to that described in Sections 5.1 and 5.2. We obtain, after very long but straightforward calculations, the homogenized relation in the final form

$$\langle D_1 \rangle = \langle \epsilon \rangle \langle E_1 \rangle + \langle g \rangle \langle H_1 \rangle, \tag{50}$$

$$\langle D_2 \rangle = \langle \epsilon \rangle \langle E_2 \rangle + \langle g \rangle \langle H_2 \rangle, \tag{51}$$

$$\langle D_3 \rangle = \epsilon_{eff} \langle E_3 \rangle + g_{eff} \langle H_3 \rangle, \tag{52}$$

$$\langle B_1 \rangle = \langle \mu \rangle \langle H_1 \rangle + \langle g \rangle \langle E_1 \rangle, \tag{53}$$

$$\langle B_2 \rangle = \langle \mu \rangle \langle H_2 \rangle + \langle g \rangle \langle E_2 \rangle, \tag{54}$$

$$\langle B_3 \rangle = \mu_{eff} \langle H_3 \rangle + g_{eff} \langle E_3 \rangle, \tag{55}$$

where the linear effective parameters ε_{eff}, μ_{eff} and g_{eff} are given by

$$\epsilon_{eff} = \frac{\left\langle \frac{\epsilon}{\epsilon\mu - g^2} \right\rangle}{\left\langle \frac{\epsilon}{\epsilon\mu - g^2} \right\rangle \left\langle \frac{\mu}{\epsilon\mu - g^2} \right\rangle - \left\langle \frac{g}{\epsilon\mu - g^2} \right\rangle^2}, \tag{56}$$

$$\mu_{eff} = \frac{\left\langle \frac{\mu}{\epsilon\mu - g^2} \right\rangle}{\left\langle \frac{\epsilon}{\epsilon\mu - g^2} \right\rangle \left\langle \frac{\mu}{\epsilon\mu - g^2} \right\rangle - \left\langle \frac{g}{\epsilon\mu - g^2} \right\rangle^2}, \tag{57}$$

$$g_{eff} = \frac{\left\langle \frac{g}{\epsilon\mu - g^2} \right\rangle}{\left\langle \frac{\epsilon}{\epsilon\mu - g^2} \right\rangle \left\langle \frac{\mu}{\epsilon\mu - g^2} \right\rangle - \left\langle \frac{g}{\epsilon\mu - g^2} \right\rangle^2}. \tag{58}$$

As before, $\langle z \rangle = \sum_{i=1}^{N} \phi_i z_i$ is the average value calculated over the sequence of layers. We observe that Eqs. (50)–(55) correspond to a transversely isotropic material where the transverse properties are given by the simple averages $\langle \epsilon \rangle, \langle \mu \rangle$ and $\langle g \rangle$, while the longitudinal ones are given by $\epsilon_{eff}, \mu_{eff}$ and g_{eff}, as reported in Eqs. (56)–(58). It is interesting to note that if $g_i = 0$ in each layer, then we have $\mu_{eff} = 1/\langle 1/\mu \rangle$, $\epsilon_{eff} = 1/\langle 1/\epsilon \rangle$ and $g_{eff} = 0$, in perfect agreement with results of Section 5.1. It is also important to remember that the energy density stored in a Tellegen medium (i.e. $1/2\mu_i \vec{H} \cdot \vec{H} + 1/2\epsilon_i \vec{E} \cdot \vec{E} + g_i \vec{E} \cdot \vec{H}$ within the i-th layer) is positive definite if $\mu_i > 0, \epsilon_i > 0$ and $g_i \leqslant \sqrt{\mu_i \epsilon_i}$, as proved by Altan (2008). These three conditions must be verified in any real layer. It is not difficult to prove that if the conditions $\mu_i > 0, \epsilon_i > 0$ and $g_i \leqslant \sqrt{\mu_i \epsilon_i}$ are verified for any $i = 1 \ldots N$, then the same conditions are verified for the effective longitudinal quantities $\epsilon_{eff}, \mu_{eff}$ and g_{eff} given in Eqs. (56)–(58), and for the effective transverse quantities $\langle \epsilon \rangle, \langle \mu \rangle$and $\langle g \rangle$. To conclude, we also underline that Eqs. (56)–(58) exhibit a curious unusual behavior: if we consider a two-layer system, we can obtain, for some combinations of parameters ϵ_i, μ_i and g_i $(i = 1, 2)$, results for $\epsilon_{eff}, \mu_{eff}$ and g_{eff} out of the intervals (ϵ_1, ϵ_1), (μ_1, μ_2) and (g_1, g_2), contrarily to most of standard homogenization rules. An example is given in Fig. 7.

6. Generalization to an arbitrary lamination direction

We prove that the previous formalism can be generalized in order to consider an arbitrary direction $\vec{n}$ of lamination. We suppose to have N different materials described by tensor $\mathcal{L}_i$ in a given coordinate system $\mathbf{e}$ (x_1, x_2, x_3). We consider another system $\mathbf{f}$ (x'_1, x'_2, x'_3), rotated with respect to $\mathbf{e}$ in order to get the axis x'_3 oriented along the unit vector $\vec{n} = (\cos\varphi \sin\vartheta, \sin\varphi \sin\vartheta, \cos\vartheta)$ on the base $\mathbf{e}$ (see Fig. 8(a)). It means that we must rotate the system $\mathbf{e}$ of an angle ϑ along the unit vector $\vec{v} = (-\sin\varphi, \cos\varphi, 0)$ (with the right-hand grip rule) (see Fig. 8(b)). To do this, we can use a rotation matrix given by the following expression (Holm, 2008)

$$\hat{\mathbb{R}}(\vartheta, \varphi) = \exp(\hat{\mathbb{V}}\vartheta) = \mathcal{I}_3 + \hat{\mathbb{V}} \sin\vartheta + \hat{\mathbb{V}}^2 (1 - \cos\vartheta) \tag{59}$$

where $\hat{\mathbb{V}}$ is the antisymmetric matrix generated by the unit vector $\vec{v}$ (it means that $\mathbb{V}_{ij} = -\varepsilon_{ijk} v_k$ where ε_{ijk} is the Levi–Civita permutation symbol). For an arbitrary vector $\vec{w}$ we have $\vec{w}^{\mathbf{e}} = \hat{\mathbb{R}}(\vartheta, \varphi)\vec{w}^{\mathbf{f}}$ where $\vec{w}^{\mathbf{e}}$ are the coordinates of $\vec{w}$ on the base $\mathbf{e}$ and $\vec{w}^{\mathbf{f}}$ are those on the base $\mathbf{f}$. This is the law of transformation of all the electric and magnetic vector fields. Explicitly, we find $\hat{\mathbb{R}}(\vartheta, \varphi)$ in the following form

$$\hat{\mathbb{R}}(\vartheta, \varphi) = \begin{pmatrix} \sin^2\varphi + \cos\vartheta \cos^2\varphi & \sin\varphi \cos\varphi(\cos\vartheta - 1) & \cos\varphi \sin\vartheta \\ \sin\varphi \cos\varphi(\cos\vartheta - 1) & \cos^2\varphi + \cos\vartheta \sin^2\varphi & \sin\varphi \sin\vartheta \\ -\cos\varphi \sin\vartheta & -\sin\varphi \sin\vartheta & \cos\vartheta \end{pmatrix}. \tag{60}$$

Concerning the strain and stress tensors we have to introduce a more complicated procedure. The following relations hold on between different frames: $\hat{\varepsilon}^{\mathbf{e}} = \hat{\mathbb{R}}(\vartheta, \varphi)\hat{\varepsilon}^{\mathbf{f}}\hat{\mathbb{R}}(\vartheta, \varphi)^T$ for the strain and, similarly, $\widehat{T}^{\mathbf{e}} = \hat{\mathbb{R}}(\vartheta, \varphi)\widehat{T}^{\mathbf{f}}\hat{\mathbb{R}}(\vartheta, \varphi)^T$ for the stress. Such expressions can be converted in Voigt notation defining two matrices $\omega_{\mathcal{T}}$ and $\omega_{\mathcal{E}}$, sometimes called Bond (1943) matrices, which acts as a rotation matrix on vectors $\mathcal{T}^T = (T_{11}, T_{22}, T_{33}, T_{23}, T_{13}, T_{12})$ and $\mathcal{E}^T = (\varepsilon_{11}, \varepsilon_{22}, \varepsilon_{33}, 2\varepsilon_{23}, 2\varepsilon_{13}, 2\varepsilon_{12})$. In other words, we can write $\mathcal{T}^{\mathbf{e}} = \omega_{\mathcal{T}}\mathcal{T}^{\mathbf{f}}$ and $\mathcal{E}^{\mathbf{e}} = \omega_{\mathcal{E}}\mathcal{E}^{\mathbf{f}}$. The entries of the matrices $\omega_{\mathcal{T}}$ and $\omega_{\mathcal{E}}$ can be easily identified by comparing $\widehat{T}^{\mathbf{e}} = \hat{\mathbb{R}}(\theta, \phi)\widehat{T}^{\mathbf{f}}\hat{\mathbb{R}}(\theta, \phi)^T$ and $\mathcal{T}^{\mathbf{e}} = \omega_{\mathcal{T}}\mathcal{T}^{\mathbf{f}}$ for the stress (and similar relations for the strain). Summing up, we can write the laws of transformation of the generalized stress

$$\mathcal{K}^{\mathbf{e}} = \begin{pmatrix} \mathcal{T}^{\mathbf{e}} \\ \vec{D}^{\mathbf{e}} \\ \vec{B}^{\mathbf{e}} \end{pmatrix} = \begin{pmatrix} \omega_{\mathcal{T}} & 0 & 0 \\ 0 & \hat{\mathbb{R}} & 0 \\ 0 & 0 & \hat{\mathbb{R}} \end{pmatrix} \begin{pmatrix} \mathcal{T}^{\mathbf{f}} \\ \vec{D}^{\mathbf{f}} \\ \vec{B}^{\mathbf{f}} \end{pmatrix} \triangleq \Omega_{\mathcal{K}}\mathcal{K}^{\mathbf{f}} \tag{61}$$

and strain

$$\mathcal{Z}^{\mathbf{e}} = \begin{pmatrix} \mathcal{E}^{\mathbf{e}} \\ -\vec{E}^{\mathbf{e}} \\ -\vec{H}^{\mathbf{e}} \end{pmatrix} = \begin{pmatrix} \omega_{\mathcal{E}} & 0 & 0 \\ 0 & \hat{\mathbb{R}} & 0 \\ 0 & 0 & \hat{\mathbb{R}} \end{pmatrix} \begin{pmatrix} \mathcal{E}^{\mathbf{f}} \\ -\vec{E}^{\mathbf{f}} \\ -\vec{H}^{\mathbf{f}} \end{pmatrix} \triangleq \Omega_{\mathcal{Z}}\mathcal{Z}^{\mathbf{f}}, \tag{62}$$

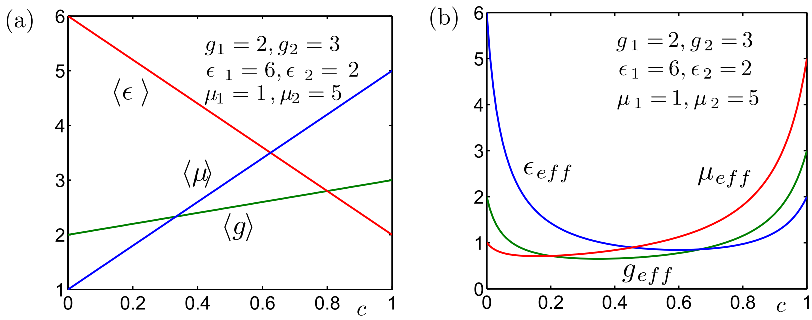

Fig. 7. Electromagnetic response of a two-layer system composed of intrinsic magneto-electric layers as function of the volume fraction c of the second layer: (a) transverse properties given by the simple averages $\langle\epsilon\rangle, \langle\mu\rangle$ and $\langle g\rangle$, (b) longitudinal properties given by $\epsilon_{eff}, \mu_{eff}$ and g_{eff}. All parameters are in arbitrary units.

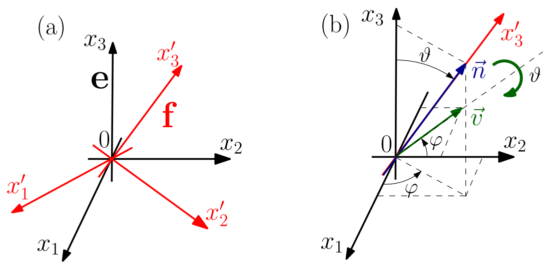

Fig. 8. Couple of coordinate systems $\mathbf{e}$ (x_1, x_2, x_3) and $\mathbf{f}$ (x_1', x_2', x_3') rotated through an orthogonal matrix $\hat{\mathbb{R}}(\theta, \phi)$ (a); the new axis x_3' is directed along the unit vector $\vec{n} = (\cos\varphi\sin\vartheta, \sin\varphi\sin\vartheta, \cos\vartheta)$. The transformation can be obtained by a rotation of an angle ϑ around the unit vector $\vec{v} = (-\sin\varphi, \cos\varphi, 0)$ (with the right-hand grip rule) lying on the plane (x_1, x_2) (b).

where we have introduced two generalized rotation matrices $\Omega_{\mathcal{K}}$ and $\Omega_{\mathcal{Z}}$. Finally, we obtain the transformation rule $\mathcal{L}_i^{\mathbf{f}} = \Omega_{\mathcal{K}}^{-1}\mathcal{L}_i^{\mathbf{e}}\Omega_{\mathcal{Z}}$ for the matrix $\mathcal{L}_i$ describing the coupled response of each material.

Now, we consider the laminated structure represented in Fig. 9. While we observe in Fig. 9(a) the cross section of each body with planes perpendicular to $\vec{n}$, we find in Fig. 9(b) the multilayer assemblage with an arbitrary lamination direction. On base $\mathbf{f}$, the direction of lamination is x_3' (see Fig. 9(b) for details) and, therefore, we can use Eq. (27) where $\mathcal{L}_i$ is substituted with $\Omega_{\mathcal{K}}^{-1}\mathcal{L}_i^{\mathbf{e}}\Omega_{\mathcal{Z}}$ (for any i) and $\mathcal{L}_{eff}$ with $\Omega_{\mathcal{K}}^{-1}\mathcal{L}_{eff}^{\mathbf{e}}\Omega_{\mathcal{Z}}$. We therefore obtain the following expression

$$\begin{aligned}\Omega_{\mathcal{K}}^{-1}\mathcal{L}_{eff}^{\mathbf{e}}\Omega_{\mathcal{Z}} = {} & \sum_{i=1}^{N}\phi_i\Omega_{\mathcal{K}}^{-1}\mathcal{L}_i^{\mathbf{e}}\Omega_{\mathcal{Z}} - \sum_{i=1}^{N}\phi_i\Omega_{\mathcal{K}}^{-1}\mathcal{L}_i^{\mathbf{e}}\Omega_{\mathcal{Z}}\mathcal{P}^T\left(\mathcal{P}\Omega_{\mathcal{K}}^{-1}\mathcal{L}_i^{\mathbf{e}}\Omega_{\mathcal{Z}}\mathcal{P}^T\right)^{-1}\mathcal{P}\Omega_{\mathcal{K}}^{-1}\mathcal{L}_i^{\mathbf{e}}\Omega_{\mathcal{Z}} \\ & + \sum_{k=1}^{N}\phi_k\Omega_{\mathcal{K}}^{-1}\mathcal{L}_k^{\mathbf{e}}\Omega_{\mathcal{Z}}\mathcal{P}^T\left(\mathcal{P}\Omega_{\mathcal{K}}^{-1}\mathcal{L}_k^{\mathbf{e}}\Omega_{\mathcal{Z}}\mathcal{P}^T\right)^{-1}\left[\sum_{i=1}^{N}\phi_i\left(\mathcal{P}\Omega_{\mathcal{K}}^{-1}\mathcal{L}_i^{\mathbf{e}}\Omega_{\mathcal{Z}}\mathcal{P}^T\right)^{-1}\right]^{-1}\sum_{j=1}^{N}\phi_j\left(\mathcal{P}\Omega_{\mathcal{K}}^{-1}\mathcal{L}_j^{\mathbf{e}}\Omega_{\mathcal{Z}}\mathcal{P}^T\right)^{-1}\mathcal{P}\Omega_{\mathcal{K}}^{-1}\mathcal{L}_j^{\mathbf{e}}\Omega_{\mathcal{Z}}.\end{aligned} \tag{63}$$

Now, we introduce the operator $\mathcal{P}_{\vec{n}}$ defined through the relations $\mathcal{P}_{\vec{n}} = \mathcal{P}\Omega_{\mathcal{K}}^{-1}$ and $\mathcal{P}_{\vec{n}}^T = \Omega_{\mathcal{Z}}\mathcal{P}^T$. We therefore obtain the final result on the original base $\mathbf{e}$

$$\begin{aligned}\mathcal{L}_{eff}^{\mathbf{e}} = {} & \sum_{i=1}^{N}\phi_i\mathcal{L}_i^{\mathbf{e}} - \sum_{i=1}^{N}\phi_i\mathcal{L}_i^{\mathbf{e}}\mathcal{P}_{\vec{n}}^T\left(\mathcal{P}_{\vec{n}}\mathcal{L}_i^{\mathbf{e}}\mathcal{P}_{\vec{n}}^T\right)^{-1}\mathcal{P}_{\vec{n}}\mathcal{L}_i^{\mathbf{e}} \\ & + \sum_{k=1}^{N}\phi_k\mathcal{L}_k^{\mathbf{e}}\mathcal{P}_{\vec{n}}^T\left(\mathcal{P}_{\vec{n}}\mathcal{L}_k^{\mathbf{e}}\mathcal{P}_{\vec{n}}^T\right)^{-1}\left[\sum_{i=1}^{N}\phi_i\left(\mathcal{P}_{\vec{n}}\mathcal{L}_i^{\mathbf{e}}\mathcal{P}_{\vec{n}}^T\right)^{-1}\right]^{-1}\sum_{j=1}^{N}\phi_j\left(\mathcal{P}_{\vec{n}}\mathcal{L}_j^{\mathbf{e}}\mathcal{P}_{\vec{n}}^T\right)^{-1}\mathcal{P}_{\vec{n}}\mathcal{L}_j^{\mathbf{e}},\end{aligned} \tag{64}$$

which is formally identical to Eq. (27).

We therefore proved that, with an arbitrary lamination direction, Eq. (27) remains unchanged provided that we use $\mathcal{P}_{\vec{n}}$ (lamination operator along $\vec{n}$) in place of $\mathcal{P}$ (lamination operator along x_3). We eventually obtain the following explicit form

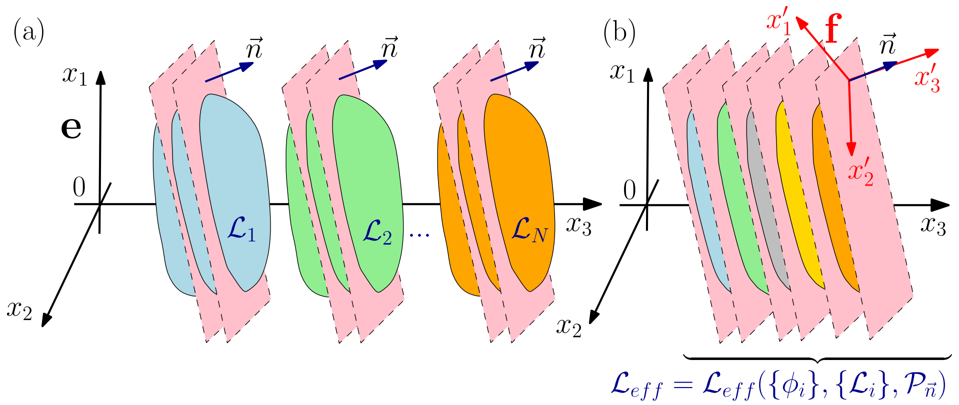

Fig. 9. Series of monocrystalline materials with properties $\mathcal{L}_i$ (measured in the base $\mathbf{e}$) sliced (or cut) by planes perpendicular to the unit vector $\vec{n}$ (a). They are later assembled to compose a multilayered structure (with effective properties $\mathcal{L}_{eff}$) with an arbitrary lamination direction (b). The base $\mathbf{f}$ with x_3' aligned with $\vec{n}$ is also represented.

$$
\mathcal{P}_{\vec{n}}^T = \begin{pmatrix}
c_\varphi^2 s_\vartheta^2 & -s_\varphi c_\varphi^2 s_\vartheta (1-c_\vartheta) & c_\varphi s_\vartheta \left(s_\varphi^2 + c_\varphi^2 c_\vartheta\right) & 0 & 0 \\
s_\varphi^2 s_\vartheta^2 & s_\varphi s_\vartheta \left(c_\varphi^2 + s_\varphi^2 c_\vartheta\right) & -s_\varphi^2 c_\varphi s_\vartheta (1-c_\vartheta) & 0 & 0 \\
c_\vartheta^2 & -s_\varphi s_\vartheta c_\vartheta & -c_\varphi s_\vartheta c_\vartheta & 0 & 0 \\
2 s_\varphi s_\vartheta c_\vartheta & s_\varphi^2 (c_\vartheta^2 - s_\vartheta^2) + c_\varphi^2 c_\vartheta & s_\varphi c_\varphi (2c_\vartheta^2 - c_\vartheta - 1) & 0 & 0 \\
2 c_\varphi s_\vartheta c_\vartheta & s_\varphi c_\varphi (2c_\vartheta^2 - c_\vartheta - 1) & c_\varphi^2 (c_\vartheta^2 - s_\vartheta^2) + s_\varphi^2 c_\vartheta & 0 & 0 \\
2 s_\varphi c_\varphi s_\vartheta^2 & c_\varphi s_\vartheta \left(c_\varphi^2 - s_\varphi^2 + 2 c_\vartheta s_\varphi^2\right) & s_\varphi s_\vartheta \left(s_\varphi^2 - c_\varphi^2 + 2 c_\vartheta c_\varphi^2\right) & 0 & 0 \\
0 & 0 & 0 & c_\varphi s_\vartheta & 0 \\
0 & 0 & 0 & s_\varphi s_\vartheta & 0 \\
0 & 0 & 0 & c_\vartheta & 0 \\
0 & 0 & 0 & 0 & c_\varphi s_\vartheta \\
0 & 0 & 0 & 0 & s_\varphi s_\vartheta \\
0 & 0 & 0 & 0 & c_\vartheta
\end{pmatrix} \tag{65}
$$

where $c_\vartheta = \cos\vartheta, c_\varphi = \cos\varphi, s_\vartheta = \sin\vartheta$ and $s_\varphi = \sin\varphi$. We remark that the generalized homogenization rule in Eq. (64) satisfies the same properties as those described in Section 4 by Eqs. (29)–(32).

In Figs. 10 and 11, we show some results obtained with the application of Eqs. (64) and (65). In Fig. 10(a) and (b), we consider configurations with two layers having orthogonal poling axes of PE and ME components in the plane (x_1, x_3). In this case, the lamination direction is orthogonal to one of the poling axes and makes a variable angle φ with the other one located in plane (x_1, x_2). In Fig. 10(c) and (d), we consider configurations with two parallel or orthogonal poling axes and a lamination direction lying in the same plane (x_1, x_3) (it makes an angle ϑ with the x_3-axis). It is interesting to note that each g_{ij} component exhibits maximum or minimum values at different specific angles φ or ϑ. This can be useful to optimize some effective properties of the overall material by changing the lamination direction. Finally, in Fig. 11 we show two modelling examples of three-layer materials. Here, as expected, we lose the symmetry (or antisymmetry) of the effective properties with respect to $\vartheta = \pi/2$; this point is clearly related to the fact that a transversely isotropic ME or PE material with a poling axis $\vec{v}$ is not coinciding with the same material with a poling axis $-\vec{v}$.

7. Graded structures

The effective response of a multilayered structure obtained above (Eqs. (27) and (64)) can be written in a more general form by introducing the averaging operator $\langle \bullet \rangle$

$$
\mathcal{L}_{eff} = \langle \mathcal{L} \rangle - \left\langle \mathcal{L}\mathcal{P}^T \left(\mathcal{P}\mathcal{L}\mathcal{P}^T\right)^{-1} \mathcal{P}\mathcal{L} \right\rangle + \left\langle \mathcal{L}\mathcal{P}^T \left(\mathcal{P}\mathcal{L}\mathcal{P}^T\right)^{-1} \right\rangle \left[\left\langle \left(\mathcal{P}\mathcal{L}\mathcal{P}^T\right)^{-1} \right\rangle \right]^{-1} \left\langle \left(\mathcal{P}\mathcal{L}\mathcal{P}^T\right)^{-1} \mathcal{P}\mathcal{L} \right\rangle. \tag{66}
$$

Here, $\mathcal{P}$ can assume either the form given in Eq. (9) or in Eq. (65). Moreover, this expression can be simply interpreted for both discrete multilayered structures (as above) and continuous or planarly graded solids, which represent the subject of the present Section. Functionally graded materials are characterized by a smooth and continuous change of physical properties along a given direction. They are typically used for mechanical applications (Miyamoto, Kaysser, Rabin, Kawasaki, & Ford, 1999), but recently their use has been extended to sensors/actuators with magneto-electro-elastic layers (Sladek, Sladek, Krahulec, & Pan, 2013). If we are dealing with a continuously stratified structure, we consider the dependence $\mathcal{L} = \mathcal{L}(x_s)$ along the lamination direction x_s corresponding to x_3, if we use $\mathcal{P}$, or to x_3' along $\vec{n}$, if we use $\mathcal{P}_{\vec{n}}$. It is not difficult to recognize that the effective tensor of a graded solid included between $x_s = 0$ and $x_s = x$ can be written in the following explicit form, where the average values of Eq. (66) are substituted by integrals

$$\mathcal{L}_{eff}(x) = \frac{1}{x}\int_0^x \mathcal{L}\,dx_s - \frac{1}{x}\int_0^x \mathcal{L}\mathcal{P}^T\left(\mathcal{P}\mathcal{L}\mathcal{P}^T\right)^{-1}\mathcal{P}\mathcal{L}\,dx_s + \frac{1}{x}\int_0^x \mathcal{L}\mathcal{P}^T\left(\mathcal{P}\mathcal{L}\mathcal{P}^T\right)^{-1}dx_s\left[\int_0^x \left(\mathcal{P}\mathcal{L}\mathcal{P}^T\right)^{-1}dx_s\right]^{-1} \times \int_0^x \left(\mathcal{P}\mathcal{L}\mathcal{P}^T\right)^{-1}\mathcal{P}\mathcal{L}\,dx_s. \tag{67}$$

In some numerical applications and theoretical developments, it can be useful to work with a differential equation describing the behavior of $\mathcal{L}_{eff}$ in terms of thickness x of the graded layer. To obtain this differential equation, we need three properties of Eq. (67):

(1) if we multiply Eq. (67) by $\mathcal{P}$ on the left and by $\mathcal{P}^T$ on the right we obtain

$$\mathcal{G}_0(x) \triangleq \left[\int_0^x \left[\mathcal{P}\mathcal{L}(x_s)\mathcal{P}^T\right]^{-1}dx_s\right]^{-1} \Rightarrow x\mathcal{G}_0(x) = \mathcal{P}\mathcal{L}_{eff}(x)\mathcal{P}^T; \tag{68}$$

(2) if we multiply Eq. (67) by $\mathcal{P}^T$ on the right we obtain

$$\mathcal{G}_1(x) \triangleq \int_0^x \mathcal{L}(x_s)\mathcal{P}^T\left[\mathcal{P}\mathcal{L}(x_s)\mathcal{P}^T\right]^{-1}dx_s \Rightarrow \frac{\mathcal{G}_1(x)}{x} = \mathcal{L}_{eff}(x)\mathcal{P}^T\left[\mathcal{P}\mathcal{L}_{eff}(x)\mathcal{P}^T\right]^{-1}; \tag{69}$$

(3) if we multiply Eq. (67) by $\mathcal{P}$ on the left we obtain

$$\mathcal{G}_2(x) \triangleq \int_0^x \left[\mathcal{P}\mathcal{L}(x_s)\mathcal{P}^T\right]^{-1}\mathcal{P}\mathcal{L}(x_s)dx_s \Rightarrow \frac{\mathcal{G}_2(x)}{x} = \left[\mathcal{P}\mathcal{L}_{eff}(x)\mathcal{P}^T\right]^{-1}\mathcal{P}\mathcal{L}_{eff}(x). \tag{70}$$

Now, considering x as an independent variable, we determine $\frac{d}{dx}\mathcal{L}_{eff}(x)$ from Eq. (67)

$$\frac{d\mathcal{L}_{eff}}{dx} = -\frac{\mathcal{L}_{eff}}{x} + \frac{\mathcal{L}}{x} - \frac{1}{x}\mathcal{L}\mathcal{P}^T\left(\mathcal{P}\mathcal{L}\mathcal{P}^T\right)^{-1}\mathcal{P}\mathcal{L} + \frac{1}{x}\frac{d\mathcal{G}_1\mathcal{G}_0\mathcal{G}_2}{dx}, \tag{71}$$

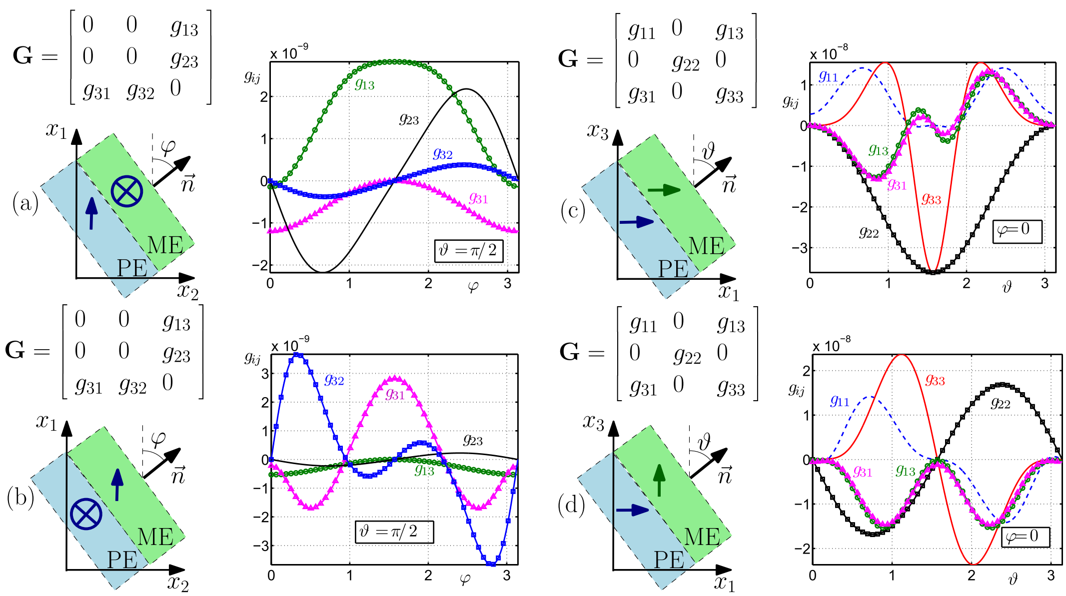

Fig. 10. Magneto-electric response of PE/ME bilayer structures as function of the lamination direction (volume fractions $\phi_1 = \phi_2 = 1/2$). In panels (a) and (b) we used $\vec{n} = (\cos\varphi, \sin\varphi, 0), 0 < \varphi < \pi$ (rad), and orthogonal poling directions aligned to x_1 and x_3. In panels (c) and (d) we adopted $\vec{n} = (\sin\vartheta, 0, \cos\vartheta), 0 < \vartheta < \pi$ (rad), and parallel or orthogonal poling directions in the plane (x_1, x_3).

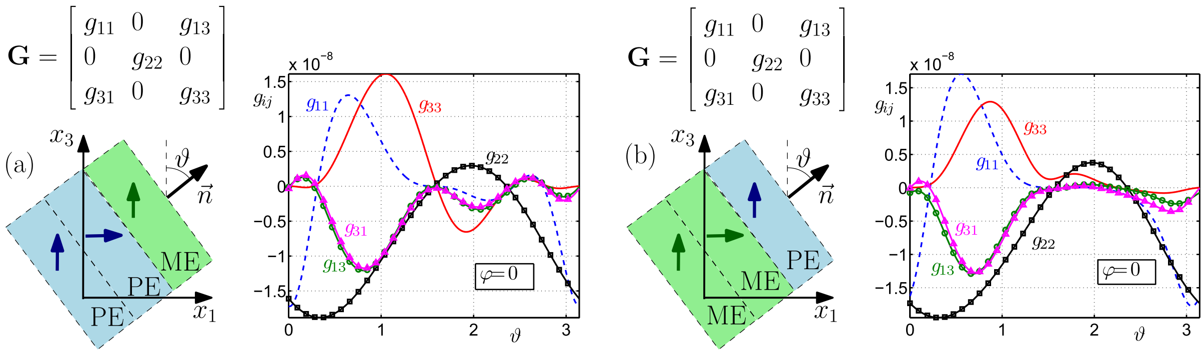

Fig. 11. Magneto-electric response of PE/ME three-layer structures as function of the lamination direction with volume fractions $\phi_1 = \phi_2 = \phi_3 = 1/3$. We adopted $\vec{n} = (\sin\vartheta, 0, \cos\vartheta)$ where $0 < \vartheta < \pi$ (rad).

where we have used the definitions in Eqs. (68)–(70). Now, by differentiating the relation $\mathcal{G}_0(x)\mathcal{G}_0(x)^{-1} = \mathcal{I}_n$ we obtain $\frac{d}{dx}\mathcal{G}_0(x) = -\mathcal{G}_0(x)\frac{d}{dx}\left[\mathcal{G}_0(x)^{-1}\right]\mathcal{G}_0(x)$ and, after some straightforward calculations based on the properties in Eqs. (68)–(70), we get the differential equation

$$x\frac{d\mathcal{L}_{eff}}{dx} = \mathcal{L} - \mathcal{L}_{eff} - (\mathcal{L} - \mathcal{L}_{eff})\mathcal{P}^T\left(\mathcal{P}\mathcal{L}\mathcal{P}^T\right)^{-1}\mathcal{P}(\mathcal{L} - \mathcal{L}_{eff}), \tag{72}$$

which describes the effective properties of a continuously stratified layer of thickness x. Of course, we need to set the initial condition $\mathcal{L}_{eff}(0) = \mathcal{L}(0)$. We remark that a substitution $z = \log x$ transforms Eq. (72) into a Riccati equation. It is interesting to note that such kind of equation was obtained to describe the behavior of other heterogeneous structures (Giordano, Palla, & Colombo, 2008; Milton, 2004).

8. Multiple-rank magneto-electro-elastic laminated materials

Multiple-rank laminated materials can be obtained by the following sequential process of lamination: dealing with two-phase materials characterized by matrices $\mathcal{L}_A$ and $\mathcal{L}_B$, we start by creating a first layered structure (along a given direction $\vec{n}_1$) composed of these materials, resulting in an effective tensor $\mathcal{L}_{AB}$. Next, we can use this composite material $\mathcal{L}_{AB}$ together with the original material $\mathcal{L}_A$ in order to obtain a rank-two laminated structure along another arbitrary direction $\vec{n}_2$. An example is shown in Fig. 12. This process can be continued until we obtain a rank-m lamination. Of course, at any stage, the existing microstructure is sliced on a length scale much larger than the previous one, in order to have well defined physical properties, which can be calculated with the preceding homogenization theory. While the idea of considering such a microstructure dates back to Maxwell (1881), more recently Tartar (1985, 2009) developed an interesting scheme for determining the permittivity tensor of such complex structures. Here, we generalize this technique in order to consider magneto-electro-elastic materials and m arbitrary sequential lamination directions. We start the analysis by observing that our initial result stated in Eq. (24) is also valid for an arbitrary lamination direction $\vec{n}$ if we adopt $\mathcal{P}_{\vec{n}}$ in place of $\mathcal{P}$. We can use Eq. (24) with $\mathcal{L}_1 = \mathcal{L}_A, \mathcal{L}_2 = \mathcal{L}_B, \phi_1 = \eta$ and $\phi_2 = 1 - \eta$. Since Eq. (24) does not effectively depend on $\mathcal{L}_0$, we can adopt $\mathcal{L}_0 = \mathcal{L}_B$ in order to simplify the result. We simply obtain

$$\mathcal{L}_{AB} = \left[\eta\mathcal{L}_A + \eta\mathcal{L}_A\mathcal{P}_{\vec{n}}^T\left(\mathcal{P}_{\vec{n}}\mathcal{L}_A\mathcal{P}_{\vec{n}}^T\right)^{-1}\mathcal{P}_{\vec{n}}(\mathcal{L}_B - \mathcal{L}_A) + (1-\eta)\mathcal{L}_B\right] \times \left[\mathcal{I}_{n+m} + \eta\mathcal{P}_{\vec{n}}^T\left(\mathcal{P}_{\vec{n}}\mathcal{L}_A\mathcal{P}^T\right)^{-1}\mathcal{P}_{\vec{n}}(\mathcal{L}_B - \mathcal{L}_A)\right]^{-1}. \tag{73}$$

This expression can be elaborated as follows: defining the quantity $\Gamma_A = \mathcal{P}_{\vec{n}}^T\left(\mathcal{P}_{\vec{n}}\mathcal{L}_A\mathcal{P}_{\vec{n}}^T\right)^{-1}\mathcal{P}_{\vec{n}}$, we obtain

$$(\mathcal{L}_{AB} - \mathcal{L}_A)[\mathcal{I}_{n+m} + \eta\Gamma_A(\mathcal{L}_B - \mathcal{L}_A)] = (1-\eta)(\mathcal{L}_B - \mathcal{L}_A). \tag{74}$$

By inverting we have

$$(\mathcal{L}_{AB} - \mathcal{L}_A)^{-1} = \frac{1}{1-\eta}(\mathcal{L}_B - \mathcal{L}_A)^{-1} + \frac{\eta}{1-\eta}\mathcal{P}_{\vec{n}}^T\left(\mathcal{P}_{\vec{n}}\mathcal{L}_A\mathcal{P}_{\vec{n}}^T\right)^{-1}\mathcal{P}_{\vec{n}}. \tag{75}$$

This expression is perfectly suited for the generalization toward the sequential multiple-rank lamination. We consider a first lamination along $\vec{n}_1$ between materials $\mathcal{L}_A$ (concentration η_1) and $\mathcal{L}_B$ (concentration $1-\eta_1$), resulting in $\mathcal{L}_{AB}$. Then, we perform a second lamination along $\vec{n}_2$ between materials $\mathcal{L}_A$ (η_2) and $\mathcal{L}_{AB}$ ($1-\eta_2$), resulting in $\mathcal{L}_{A(AB)}$. Next, we consider a third lamination along $\vec{n}_3$ between $\mathcal{L}_A$ (η_3) and $\mathcal{L}_{A(AB)}$ ($1-\eta_3$), resulting in $\mathcal{L}_{A(A(AB))}$, and so on until the m-th step. We can write one homogenization rule for each lamination stage

$$\left(\mathcal{L}_{AB}-\mathcal{L}_A\right)^{-1}=\frac{1}{1-\eta_1}\left(\mathcal{L}_B-\mathcal{L}_A\right)^{-1}+\frac{\eta_1}{1-\eta_1}\mathcal{P}^T_{\vec{n}_1}\left(\mathcal{P}_{\vec{n}_1}\mathcal{L}_A\mathcal{P}^T_{\vec{n}_1}\right)^{-1}\mathcal{P}_{\vec{n}_1}, \tag{76}$$

$$\left(\mathcal{L}_{A(AB)}-\mathcal{L}_A\right)^{-1}=\frac{1}{1-\eta_2}\left(\mathcal{L}_{AB}-\mathcal{L}_A\right)^{-1}+\frac{\eta_2}{1-\eta_2}\mathcal{P}^T_{\vec{n}_2}\left(\mathcal{P}_{\vec{n}_2}\mathcal{L}_A\mathcal{P}^T_{\vec{n}_2}\right)^{-1}\mathcal{P}_{\vec{n}_2}, \tag{77}$$

$$\left(\mathcal{L}_{A(A(AB))}-\mathcal{L}_A\right)^{-1}=\frac{1}{1-\eta_3}\left(\mathcal{L}_{A(AB)}-\mathcal{L}_A\right)^{-1}+\frac{\eta_3}{1-\eta_3}\mathcal{P}^T_{\vec{n}_3}\left(\mathcal{P}_{\vec{n}_3}\mathcal{L}_A\mathcal{P}^T_{\vec{n}_3}\right)^{-1}\mathcal{P}_{\vec{n}_3},\ldots \tag{78}$$

$$\left(\mathcal{L}_{\underbrace{A(A(\ldots(AB)))}_{m\ \text{times}}}-\mathcal{L}_A\right)^{-1}=\frac{1}{1-\eta_m}\left(\mathcal{L}_{\underbrace{A(A(\ldots(AB)))}_{(m-1)\ \text{times}}}-\mathcal{L}_A\right)^{-1}+\frac{\eta_m}{1-\eta_m}\mathcal{P}^T_{\vec{n}_m}\left(\mathcal{P}_{\vec{n}_m}\mathcal{L}_A\mathcal{P}^T_{\vec{n}_m}\right)^{-1}\mathcal{P}_{\vec{n}_m}. \tag{79}$$

A simple iterative composition of these equations leads to the final result

$$\left(\mathcal{L}_{\underbrace{A(A(\ldots(AB)))}_{m\ \text{times}}}-\mathcal{L}_A\right)^{-1}=\xi_0\left(\mathcal{L}_B-\mathcal{L}_A\right)^{-1}+\sum_{k=1}^{m}\xi_k\mathcal{P}^T_{\vec{n}_k}\left(\mathcal{P}_{\vec{n}_k}\mathcal{L}_A\mathcal{P}^T_{\vec{n}_k}\right)^{-1}\mathcal{P}_{\vec{n}_k}, \tag{80}$$

where

$$\xi_0=\prod_{k=1}^{m}\frac{1}{1-\eta_k}\quad\text{and}\quad\xi_k=\eta_k\prod_{j=k}^{m}\frac{1}{1-\eta_j}. \tag{81}$$

It is interesting to observe that the final volume fraction of $\mathcal{L}_B$ is given by $\eta_B=1/\xi_0$; similarly, the final volume fraction of $\mathcal{L}_A$ is $\eta_A=1-1/\xi_0$. To conclude, we have generalized the Tartar (1985, 2009) formula to magneto-electro-elastic multi-laminated systems with an arbitrary set of lamination directions $\vec{n}_1,\ldots,\vec{n}_m$. As before, the final result is ground on our definition of the arbitrary lamination tensor $\mathcal{P}_{\vec{n}}$, reported in Eq. (65).

We describe now a series of relevant applications of the theory. We consider some two-dimensional structures with a rank-two lamination geometry. They can be found in Fig. 13 where their diagram and the corresponding magneto-electric response are reported. For a rank-two configuration having volume fractions η_1 and η_2, the final volume fraction of the component A is given by $\eta_A=1-(1-\eta_1)(1-\eta_2)=\eta_1+\eta_2-\eta_1\eta_2$. If we impose $\eta_A=1/2$ we have $\eta_1=(1/2-\eta_2)/(1-\eta_2)$ or, equivalently, $\eta_2=(1/2-\eta_1)/(1-\eta_1)$. Therefore, in Fig. 13 we assumed $\eta_1=c$ and $\eta_2=(1/2-c)/(1-c)$ where $0<c<1/2$. Moreover, we used orthogonal lamination directions $\vec{n}_1$ along x_1 and $\vec{n}_2$ along x_2. The first configuration is characterized by poling directions along x_1 and the second one by poling directions along x_2. We note that the first structure for $c=0$ and the second one for $c=1/2$ correspond to the system in Fig. 2(b); similarly, the first structure for $c=1/2$ and the second one for $c=0$ correspond to the system in Fig. 2(a). Indeed, the values of the magneto-electric coefficients for $c=0$ and $c=1/2$ are in perfect agreement with Fig. 2(a) and (b). It is interesting to remark that such configurations exhibit a linear dependence of g_{33} as function of c. This property can be exploited to design a material with highly precise values of the magneto-electric parameter g_{33}. Now, we consider some examples with varying lamination directions. In Fig. 14, four configurations have been shown: (a) $\vec{n}_1=(\cos\varphi_1,\sin\varphi_1,0),\vec{n}_2=(0,1,0)$, PE$//x_1$ and ME $//x_1$; (b) $\vec{n}_1=(\cos\varphi_1,\sin\varphi_1,0),\vec{n}_2=(0,1,0)$, PE$//x_2$ and ME $//x_2$; (c) $\vec{n}_1=(1,0,0),\vec{n}_2=(\cos\varphi_2,\sin\varphi_2,0)$, PE$//x_1$ and ME $//x_1$; (d) $\vec{n}_1=(1,0,0),\vec{n}_2=(\cos\varphi_2,\sin\varphi_2,0)$, PE$//x_2$ and ME $//x_2$. In all cases we imposed $\eta_A=1/2$ and $\eta_1=\eta_2$. Since $\eta_A=\eta_1+\eta_2-\eta_1\eta_2$ we obtained the volume fractions $\eta_1=\eta_2=(2-\sqrt{2})/2$. Case (a) and (b) with $\varphi_1=0$ and case (c) and (d) with $\varphi_2=\pi/2$ correspond to Fig. 13 with $c=(2-\sqrt{2})/2$. Case (a) with $\varphi_1=\pi/2$ and case (d) with $\phi_2=0$ correspond to Fig. 2(b) with $c=1/2$. Finally, case (b) with $\varphi_1=\pi/2$ and case (c) with $\phi_2=0$ correspond to Fig. 2(a) with $c=1/2$.

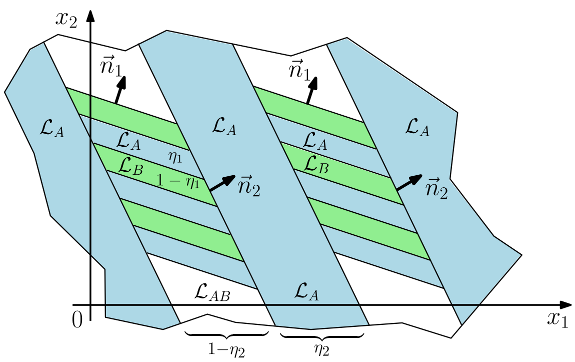

Fig. 12. Scheme of a rank-two laminated material composed of components $\mathcal{L}_A$ and $\mathcal{L}_B$. The first stage is described by the lamination direction $\vec{n}_1$ and the volume fraction η_1; the second one by $\vec{n}_2$ and η_2. The overall effective tensor $\mathcal{L}_{A(AB)}$ depends on $\mathcal{L}_A,\mathcal{L}_B,\vec{n}_1,\eta_1,\vec{n}_2$ and η_2, as explicitly shown in Eq. (80). Higher-rank laminations can be simply obtained by further iterations.

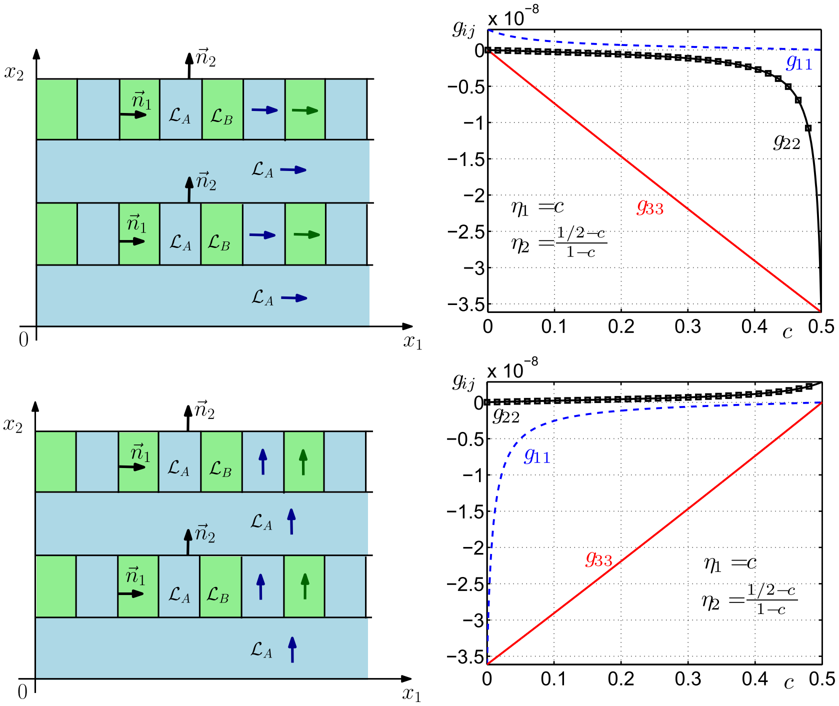

Fig. 13. Rank-two multilayer materials with orthogonal lamination directions $\vec{n}_1//x_1$ and $\vec{n}_2//x_2$. Two configurations correspond to different alignment of the poling axes: PE ($\mathcal{L}_A$) and ME ($\mathcal{L}_B$) $//x_1$(top); PE ($\mathcal{L}_A$) and ME ($\mathcal{L}_B$) $//x_2$(bottom).

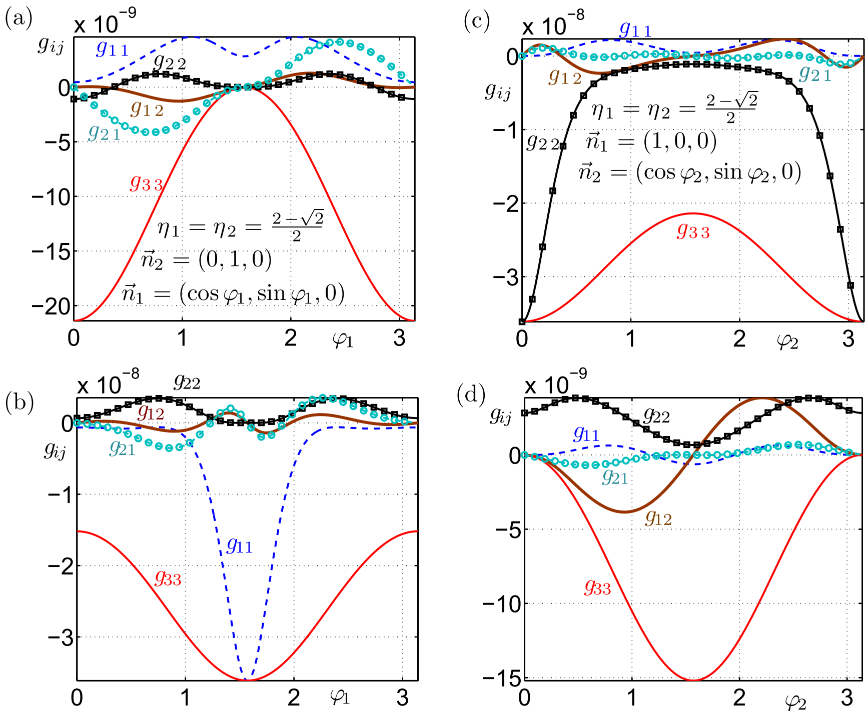

Fig. 14. Effective magnetoelectric response of four configurations of rank-two multilayer materials with varying lamination directions: (a) $\vec{n}_1 = (\cos\varphi_1, \sin\varphi_1, 0), \vec{n}_2 = (0, 1, 0)$, PE$//x_1$ and ME $//x_1$; (b) $\vec{n}_1 = (\cos\varphi_1, \sin\varphi_1, 0), \vec{n}_2 = (0, 1, 0)$, PE$//x_2$ and ME $//x_2$; (c) $\vec{n}_1 = (1, 0, 0), \vec{n}_2 = (\cos\varphi_2, \sin\varphi_2, 0)$, PE$//x_1$ and ME $//x_1$; (d) $\vec{n}_1 = (1, 0, 0), \vec{n}_2 = (\cos\varphi_2, \sin\varphi_2, 0)$, PE$//x_2$ and ME $//x_2$. Everywhere we adopted $\eta_1 = \eta_2 = (2-\sqrt{2})/2$ and the angles are in radians.

To conclude, we add some comments on the practical use of the effective tensor in real structures. The final overall properties of the laminated system can be written as

$$\langle\mathcal{K}\rangle = \begin{pmatrix} \langle\mathcal{T}\rangle \\ \left\langle\vec{D}\right\rangle \\ \left\langle\vec{B}\right\rangle \end{pmatrix} = \begin{pmatrix} \mathbf{C} & \mathbf{E} & \mathbf{F} \\ \mathbf{E}^T & -\mathbf{P} & -\mathbf{G} \\ \mathbf{F}^T & -\mathbf{G}^T & -\mathbf{M} \end{pmatrix} \begin{pmatrix} \langle\mathcal{E}\rangle \\ -\left\langle\vec{E}\right\rangle \\ -\left\langle\vec{H}\right\rangle \end{pmatrix} = \mathcal{L}_{eff}\langle\mathcal{Z}\rangle \tag{82}$$

where $\mathcal{L}_{eff}$, or all submatrices of $\mathcal{L}_{eff}$, can be found with one of the procedures described in the present paper. If we are interested in the electromagnetic response of the system, we can adopt two different types of boundary conditions from the elastic point of view: (i) a mechanically clamped structure (i.e. $\langle\mathcal{E}\rangle = 0$) leads to the relationships $\left\langle\vec{D}\right\rangle = \mathbf{P}\left\langle\vec{E}\right\rangle + \mathbf{G}\left\langle\vec{H}\right\rangle$ and $\left\langle\vec{B}\right\rangle = \mathbf{G}^T\left\langle\vec{E}\right\rangle + \mathbf{M}\left\langle\vec{H}\right\rangle$; (ii) a mechanically free structure (i.e. $\langle\mathcal{T}\rangle = 0$) is described by the relations $\left\langle\vec{D}\right\rangle = (\mathbf{P} + \mathbf{E}^T\mathbf{C}^{-1}\mathbf{E})\left\langle\vec{E}\right\rangle + (\mathbf{G} + \mathbf{E}^T\mathbf{C}^{-1}\mathbf{F})\left\langle\vec{H}\right\rangle$ and $\left\langle\vec{B}\right\rangle = (\mathbf{G}^T + \mathbf{F}^T\mathbf{C}^{-1}\mathbf{E})\left\langle\vec{E}\right\rangle + (\mathbf{M} + \mathbf{F}^T\mathbf{C}^{-1}\mathbf{F})\left\langle\vec{H}\right\rangle$. So, once the elastic boundary conditions are defined, we can obtain a pure electromagnetic effective constitutive relation. Usually, this procedure is used to characterize the behavior of magnetoelectric devices, as largely described by Bichurin et al. (2010a, 2010b).

9. Conclusions

In the present work, we described a comprehensive homogenization technique for determining the tensor properties of a laminated material. In particular, we analysed the magneto-electro-elastic coupled behavior of laminated artificial multiferroics. The most relevant aspect of the theory is its capability to homogenize the structure for an arbitrary lamination direction. To this aim, we introduced an *ad hoc* lamination tensor $\mathcal{P}_{\vec{n}}$, which is presented in closed form and therefore is easily implementable in any software code used to determine the response of a heterogeneous system. Moreover, the possibility to consider an arbitrary lamination direction allowed for generalizing our formalism to functionally graded and multiple-rank laminated structures. Interestingly, the final effective tensor automatically exhibits the correct symmetries generated by the combination of all the anisotropic characters of involved layers. Finally, we proved that the cut of interfaces with a given orientation allows us to obtain composite systems with complex responses. This last point can be thoroughly exploited to design a material with specific desired properties.

Appendix A. Properties of transversely isotropic materials

A transversely isotropic magneto-electro-elastic material is described by the following tensor

$$\mathcal{L} = \begin{bmatrix} c_{11} & c_{12} & c_{13} & 0 & 0 & 0 & 0 & 0 & e_{31} & 0 & 0 & f_{31} \\ c_{12} & c_{11} & c_{13} & 0 & 0 & 0 & 0 & 0 & e_{31} & 0 & 0 & f_{31} \\ c_{13} & c_{13} & c_{33} & 0 & 0 & 0 & 0 & 0 & e_{33} & 0 & 0 & f_{33} \\ 0 & 0 & 0 & c_{44} & 0 & 0 & 0 & e_{15} & 0 & 0 & f_{15} & 0 \\ 0 & 0 & 0 & 0 & c_{44} & 0 & e_{15} & 0 & 0 & f_{15} & 0 & 0 \\ 0 & 0 & 0 & 0 & 0 & \frac{c_{11}-c_{12}}{2} & 0 & 0 & 0 & 0 & 0 & 0 \\ 0 & 0 & 0 & 0 & e_{15} & 0 & -p_{11} & 0 & 0 & -g_{11} & 0 & 0 \\ 0 & 0 & 0 & e_{15} & 0 & 0 & 0 & -p_{11} & 0 & 0 & -g_{11} & 0 \\ e_{31} & e_{31} & e_{33} & 0 & 0 & 0 & 0 & 0 & -p_{33} & 0 & 0 & -g_{33} \\ 0 & 0 & 0 & 0 & f_{15} & 0 & -g_{11} & 0 & 0 & -m_{11} & 0 & 0 \\ 0 & 0 & 0 & f_{15} & 0 & 0 & 0 & -g_{11} & 0 & 0 & -m_{11} & 0 \\ f_{31} & f_{31} & f_{33} & 0 & 0 & 0 & 0 & 0 & -g_{33} & 0 & 0 & -m_{33} \end{bmatrix} \tag{A.1}$$

where we adopted these notations for the physical parameters: c_{ij} are the elastic stiffness constants, p_{ij} the electric permittivities, m_{ij} the magnetic permeabilities, e_{ij} the piezoelectric coefficients, f_{ij} the magnetoelastic coefficients, and g_{ij} the magnetoelectric coefficients. In this paper; we used two materials belonging to this crystal class: the barium titanate piezoelectric ceramic $BaTiO_3$ described by the following parameters

$$\begin{aligned}
&c_{a11} = 166\times10^9\ \text{Pa}, \quad c_{a12} = 77\times10^9\ \text{Pa}, \quad c_{a13} = 78\times10^9\ \text{Pa}, \\
&c_{a33} = 162\times10^9\ \text{Pa}, \quad c_{a44} = 43\times10^9\ \text{Pa}, \quad p_{a11} = 11.1\times10^{-9}\ \text{C}^2/(\text{Nm}^2), \\
&p_{a33} = 12.6\times10^{-9}\ \text{C}^2/(\text{Nm}^2), \quad m_{a11} = 5\times10^{-6}\ \text{N/A}^2, \quad m_{a33} = 10\times10^{-6}\ \text{N/A}^2, \\
&e_{a31} = -4.4\ \text{C/m}^2, \quad e_{a15} = 11.6\ \text{C/m}^2, \quad e_{a33} = 18.6\ \text{C/m}^2, \\
&f_{a31} = f_{a15} = f_{a33} = 0\ \text{N/(Am)}, \quad g_{a11} = g_{a33} = 0\ \text{s/m}
\end{aligned}$$

and the cobalt ferrite magnetoelastic material $CoFe_2O_4$ with parameters

$$c_{b11} = 286 \times 10^9 \text{ Pa}, \quad c_{b12} = 173 \times 10^9 \text{ Pa}, \quad c_{b13} = 170 \times 10^9 \text{ Pa},$$
$$c_{b33} = 269.5 \times 10^9 \text{ Pa}, \quad c_{b44} = 45.3 \times 10^9 \text{ Pa}, \quad p_{b11} = 0.08 \times 10^{-9} \text{ C}^2/(\text{Nm}^2),$$
$$p_{b33} = 0.093 \times 10^{-9} \text{ C}^2/(\text{Nm}^2), \quad m_{b11} = 590 \times 10^{-6} \text{ N/A}^2, \quad m_{b33} = 157 \times 10^{-6} \text{ N/A}^2,$$
$$e_{b31} = e_{b15} = e_{b33} = 0 \text{ C/m}^2, \quad g_{b11} = g_{b33} = 0 \text{ s/m},$$
$$f_{b31} = 580.3 \text{ N/(Am)}, \quad f_{b15} = 550 \text{ N/(Am)}, f_{b33} = -699.7 \text{ N/(Am)}.$$

As was noted by Sun and Kim (2010) (and later by Kim (2011)), signs for m_{b11} and f_{b33} of the cobalt ferrite are incorrect in most of the existing literature. In the present paper, the correct values were used in numerical calculations. We remark that the piezomagnetic coefficients (third order tensor) of the cobalt ferrite represent the linearization of the magnetostrictive behavior (fourth order tensor) around a specific value of an applied bias magnetic field (along the poling direction). Normally, the bias magnetic field corresponds to the inflection point of the curve representing the elastic deformation versus the applied magnetic field: it coincides with the higher slope or, equivalently, with the stronger magneto-elastic coupling.

References

Altan, B. S. (2008). A Uniqueness theorem for initial-boundary value problems in Tellegen medium. *Progress In Electromagnetics Research C, 1*, 73–85.
Avellaneda, M., & Harshé, G. (1994). Magnetoelectric effect piezoelectric/magnetostrictive multilayer (2-2) composites. *Journal of Intelligent Material Systems and Structures, 5*, 501–513.
Avellaneda, M., & Olson, T. (1993). Effective medium theories and effective electromechanical coupling factors for piezoelectric composites. *Journal of Intelligent Material Systems and Structures, 4*, 82–88.
Backus, G. E. (1962). Long-wave elastic anisotropy produced by horizontal layering. *Journal of Geophysical Research, 67*, 4427–4440.
Bichurin, M. I., Petrov, V. M., Averkin, S. V., & Liverts, E. (2010a). Present status of theoretical modeling the magnetoelectric effect in magnetostrictive-piezoelectric nanostructures. Part I: Low frequency and electromechanical resonance ranges. *Journal of Applied Physics, 107*, 053904.
Bichurin, M. I., Petrov, V. M., Averkin, S. V., & Liverts, E. (2010b). Present status of theoretical modeling the magnetoelectric effect in magnetostrictive-piezoelectric nanostructures. Part II: Magnetic and magnetoacoustic resonance ranges. *Journal of Applied Physics, 107*, 053905.
Bond, W. (1943). The mathematics of the physical properties of crystals. *The Bell System Technical Journal, 22*, 1–72.
Bravo-Castillero, J., Rodríguez-Ramos, R., Mechkour, H., Otero, J. A., & Sabina, F. J. (2008). Homogenization of magneto-electro-elastic multilaminated materials. *The Quarterly Journal of Mechanics and Applied Mathematics, 61*, 311–332.
Brenner, R. (2009). Numerical computation of the response of piezoelectric composites using Fourier transform. *Physical Review B, 79*, 184106.
Challagulla, K. S., & Georgiades, A. V. (2011). Micromechanical analysis of magneto-electro-thermo-elastic composite materials with applications to multilayered structures. *International Journal of Engineering Science, 49*, 85–104.
Colombo, L., & Giordano, S. (2011). Nonlinear elasticity in nanostructured materials. *Reports on Progress in Physics, 74*, 116501.
Corcolle, R., Daniel, L., & Bouillault, F. (2008). Generic formalism for homogenization of coupled behavior: Application to magnetoelectroelastic behavior. *Physical Review B, 78*, 214110.
Dusch, Y., Tiercelin, N., Klimov, A., Giordano, S., Preobrazhensky, V., & Pernod, P. (2013). Stress-mediated magnetoelectric memory effect with uniaxial $TbCo_2$/FeCo multilayer on 011-cut PMN-PT ferroelectric relaxor. *Journal of Applied Physics, 113*, 17C719.
Eerenstein, W., Mathur, N. D., & Scott, J. F. (2006). Multiferroic and magnetoelectric materials. *Nature, 442*, 759–765.
Eshelby, J. D. (1957). The determination of the elastic field of an ellipsoidal inclusion, and related problems. *Proceedings of the Royal Society London, A241*, 376–396.
Fetisov, L. Y., Perov, N. S., Fetisov, Y. K., Srinivasan, G., & Petrov, V. M. (2011). Resonance magnetoelectric interactions in an asymmetric ferromagnetic-ferroelectric layered structure. *Journal of Applied Physics, 109*, 053908.
Fiebig, M. (2005). Revival of the magnetoelectric effect. *Journal of Physics D: Applied Physics, 38*, R123–R152.
Francfort, G. A., & Murat, F. (1986). Homogenization and optimal bounds in linear elasticity. *Archive for Rational Mechanics and Analysis, 94*, 307–334.
Gibiansky, L. V., & Torquato, S. (1999). Matrix laminate composites: Realizable approximations for the effective moduli of piezoelectric dispersions. *Journal of Materials Research, 14*, 49–63.
Giordano, S. (2005). Order and disorder in heterogeneous material microstructure: Electric and elastic characterization of dispersions of pseudo oriented spheroids. *International Journal of Engineering Science, 43*, 1033–1058.
Giordano, S. (2007). Relation between microscopic and macroscopic mechanical properties in random mixtures of elastic media. *Journal of Engineering Materials and Technology, 129*, 453–461.
Giordano, S., Dusch, Y., Tiercelin, N., Pernod, P., & Preobrazhensky, V. (2012). Combined nanomechanical and nanomagnetic analysis of magnetoelectric memories. *Physical Review B, 85*, 155321.
Giordano, S., & Palla, P. L. (2008). Dielectric behavior of anisotropic inhomogeneities: Interior and exterior points Eshelby tensors. *Journal of Physics A: Mathematical and Theoretical, 41*, 415205.
Giordano, S., Palla, P. L., & Colombo, L. (2008). Effective permittivity of materials containing graded ellipsoidal inclusions. *The European Physical Journal B, 66*, 29–35.
Holm, D. D. (2008). *Geometric mechanics, Part I and II*. London: World Scientific.
Huang, J. H., Chiu, Y. H., & Liu, H. K. (1998). Magneto-electro-elastic Eshelby tensors for a piezoelectric–piezomagnetic composite reinforced by ellipsoidal inclusions. *Journal of Applied Physics, 83*, 5364–5369.
Huang, J. H., & Kuo, W. S. (1997). The analysis of piezoelectric/piezomagnetic composite materials containing ellipsoidal inclusions. *Journal of Applied Physics, 81*, 1378–1386.
Kachanov, M., & Sevostianov, I. (2005). On quantitative characterization of microstructures and effective properties Original. *International Journal of Solids and Structures, 42*, 309–336.
Kim, J. Y. (2011). Micromechanical analysis of effective properties of magneto-electro-thermo-elastic multilayer composites. *International Journal of Engineering Science, 49*, 1001–1018.
Kuo, H.-Y., & Pan, E. (2011). Effective magnetoelectric effect in multicoated circular fibrous multiferroic composites. *Journal of Applied Physics, 109*, 104901.
Landau, L. D., & Lifshitz, E. M. (1986). *Theory of elasticity*. Oxford: Butterworths Heinemann.
Landau, L. D., Pitaevskii, L. P., & Lifshitz, E. M. (1984). *Electrodynamics of continuous media*. Oxford: Butterworths Heinemann.
Lawes, G., & Srinivasan, G. (2011). Introduction to magnetoelectric coupling and multiferroic films. *Journal of Physics D: Applied Physics, 44*, 243001.
Maxwell, J. C. (1881). *A treatise on electricity and magnetism*. Oxford: Clarendon.
Milton, G. W. (1990). On characterizing the set of possible effective tensors of composites: The variational method and the translation method. *Communications on Pure and Applied Mathematics, 43*, 63–125.
Milton, G. W. (2004). *The theory of composites*. Cambridge: Cambridge University Press.

Miyamoto, Y., Kaysser, W. A., Rabin, B. H., Kawasaki, A., & Ford, R. G. (1999). *Functionally graded materials: Design, processing and applications*. Boston, MA: Kluwer Academic Publishers.
Nan, C. W., Bichurin, M. I., Dong, S., Viehland, D., & Srinivasan, G. (2008). Multiferroic magnetoelectric composites: Historical perspective, status, and future directions. *Journal of Applied Physics, 103*, 031101.
Nye, J. F. (1985). *Physical properties of cristals: Their representation by tensors and matrices*. Oxford: Oxford University Press.
Palla, P. L., Giordano, S., & Colombo, L. (2010). Lattice model describing scale effects in nonlinear elasticity of nanoinhomogeneities. *Physical Review B, 81*, 214113.
Postma, G. W. (1955). Waves propagation in a stratified medium. *Geophysics, 20*, 780–806.
Ramesh, R., & Spaldin, N. A. (2007). Multiferroics: Progress and prospects in thin films. *Nature Materials, 6*, 21–29.
Ramirez, F., Heyliger, P. R., & Pan, E. (2006). Discrete layer solution to free vibrations of functionally graded magneto-electro-elastic plate. *Mechanics of Advanced Materials and Structures, 13*, 249–266.
Roy, K., Bandyopadhyay, S., & Atulasimha, J. (2011). Hybrid spintronics and straintronics: A magnetic technology for ultra low energy computing and signal processing. *Applied Physics Letters, 99*, 063108.
Sihvola, A. H. (1994). Electromagnetic modeling of bi-isotropic media. *Progress in Electromagnetic Research, 9*, 45–86.
Sirotine, Y., & Chaskolskaia, M. (1984). *Fondaments de la physique des cristaux*. Moscou: Editions MIR.
Sixto-Camacho, L. M., Bravo-Castillero, J., Brenner, R., Guinovart-Díaz, R., Mechkourd, H., Rodríguez-Ramos, R., et al (2013). Asymptotic homogenization of periodic thermo-magneto-electro-elastic heterogeneous media. *Computers and Mathematics with Applications, 66*, 2056–2074.
Sladek, J., Sladek, V., Krahulec, S., & Pan, E. (2013). Analyses of functionally graded plates with a magnetoelectroelastic layer. *Smart Materials and Structures, 22*, 035003.
Sun, K. H., & Kim, Y. Y. (2010). Layout design optimization for magneto-electro-elastic laminate composites for maximized energy conversion under mechanical loading. *Smart Materials and Structures, 19*, 055008.
Tartar, L. (1979). Estimation de coefficients homogénéisés. In R. Glowinski & J. L. Lions (Eds.), *Computing methods in applied sciences and engineering* (pp. 364–373). Berlin: Springer-Verlag.
Tartar, L. (1985). Estimations fines des coefficients homogénéisés. In P. Krée (Ed.), *Ennio de Giorgi colloquium: Papers presented at a colloquium held at the H. Poincaré Institute in November 1983* (pp. 168–187). London: Pitman Publishing Ltd..
Tartar, L. (2009). *The general theory of homogenization: A personalized introduction*. Berlin: Springer-Verlag.
Tiercelin, N., Dusch, Y., Klimov, A., Giordano, S., Preobrazhensky, V., & Pernod, P. (2011). Room temperature magnetoelectric memory cell using stress-mediated magnetoelastic switching in nanostructured multilayers. *Applied Physics Letters, 99*, 192507.
Tiercelin, N., Preobrazhensky, V., Pernod, P., & Ostaschenko, A. (2008b). Enhanced magnetoelectric effect in nanostructured magnetostrictive thin film resonant actuator with field induced spin reorientation transition. *Applied Physics Letters, 92*, 062904.
Tiercelin, N., Talbi, A., Preobrazhensky, V., Pernod, P., Mortet, V., Haenen, K., et al (2008a). Magnetoelectric effect near spin reorientation transition in giant magnetostrictive-aluminum nitride thin film structure. *Applied Physics Letters, 93*, 162902.
Torquato, S. (2002). *Random heterogeneous materials: Microstructure and macroscopic properties*. New York: Springer-Verlag.
van den Boomgaard, J., & Born, R. A. J. (1978). A sintered magnetoelectric composite material $BaTiO_3$–Ni(Co,Mn)Fe_2O_4. *Journal of Materials Science, 13*, 1538–1548.
Wang, Y., Hu, J., Lin, Y., & Nan, C. W. (2010). Multiferroic magnetoelectric composite nanostructures. *NPG Asia Materials, 2*, 61–68.
Zhai, J., Xing, Z., Dong, S., Li, J., & Viehland, D. (2008). Magnetoelectric laminated composites: An overview. *Journal of the American Ceramic Society, 91*, 351–358.